Hiroshima University Doctoral Thesis

Modulation of Stress-Responsive Rapid Production of the Phytohormone Abscisic Acid *via* Endoplasmic Reticulum Dynamics

（ストレスに応答したアブシシン酸の迅速生成の
小胞体ダイナミクスを介した調節に関する研究）

2020
Department of Mathematical and Life Sciences,
Graduate School of Science,
Hiroshima University
Yiping HAN

Thesis index

1. Main Thesis

Modulation of Stress-Responsive rapid Production of the Phytohormone Abscisic Acid *via* Endoplasmic Reticulum Dynamics
（ストレスに応答したアブシシン酸の迅速生成の小胞体ダイナミクスを介した調節に関する研究）

2. Article

Dynamics of the leaf endoplasmic reticulum modulate ß-glucosidase-mediated stress-activated ABA production from its glucosyl ester*
Yiping Han, Shunsuke Watanabe, Hiroshi Shimada and Atsushi Sakamoto
Journal of Experimental Botany, accepted for publication
DOI:10.1093/jxb/erz528

*Original paper in a peer-reviewed journal

Main Thesis

DOCTORAL THESIS

Modulation of Stress-Responsive Rapid Production of the Phytohormone Abscisic Acid *via* Endoplasmic Reticulum Dynamics

2020
Department of Mathematical and Life Sciences,
Graduate School of Science,
Hiroshima University
Yiping HAN

DECLARATION OF CO-AUTHORSHIP/PREVIOUS PUBLICATION

I. Co-Authorship Declaration

I hereby declare that this thesis incorporates material from joint research. I certify that I have essentially done all the work and obtained written permission from each of the co-authors to include the above material in my thesis. I certify that, with the above qualification, this thesis and the work to which it refers are the results of my own efforts.

II. Declaration of Previous Publication

This thesis includes one original paper that has been published in a peer-reviewed journal:

Authors: Yiping Han, Shunsuke Watanabe, Hiroshi Shimada and Atsushi Sakamoto
Article title: Dynamics of the leaf endoplasmic reticulum modulate ß-glucosidase-mediated stress-activated ABA production from its glucosyl ester.
Journal: *Journal of Experimental Botany*, in press
Publisher: Oxford University Press
DOI: 10.1093/jxb/erz528
Article first published online: 25 November 2019
Accepted manuscript online: 20 November 2019

 It is noted that, where it was necessary, the original text is slightly modified to fit the formatting and structuring style of the thesis. I certify that the above material describes work completed during my registration as graduate student at Hiroshima University.

Contents

Abbreviations

ABA .....abscisic acid
ABAld .....ABA aldehyde
ABA-GE .....ABA-glucose ester
ALN .....allantoinase
ANOVA .....analysis of variance
BiP .....binding protein
BGLU .....β-glucosidase
DW .....dry weight
ER .....endoplasmic reticulum
FW .....fresh weight
GFP .....green fluorescent protein
IPP .....isopentenyl pyrophosphate
LB .....left border
LC-ESI-MS/MS .....liquid chromatography-electrospray ionization-tandem mass spectrometry
MeJA .....methyl jasmonate
mRFP .....monomeric red fluorescent protein
NCED .....nine-*cis*-epoxycarotenoid dioxygenase
PAGE .....polyacrylamide gel electrophoresis
PCR .....polymerase chain reaction
PEG .....polyethylene glycol
PPR .....pentatricoeptide repeat
RBC .....ribulose-1,5-bisphosphate carboxylase/oxygenase
RBCL .....RBC large subunits
RD .....responsive to desiccation
RT-qPCR .....reverse transcription-quantitative PCR
RWC .....relative water content
SDS .....sodium dodecyl sulfate
T-DNA .....transferred DNA
TAIR .....The Arabidopsis Information Resource
TW .....turgid weight
UBC .....ubiquitin-conjugatin enzyme
WT .....wild type
ZEP..... zeaxanthin epoxidase

GENERAL INTRODUCTION

Stress response and defense system in plants

Owing to their great contribution to the fixation of solar energy, adjustment of atmospheric composition, and nutrient circulation, plants serve as an indispensable element of the terrestrial ecosphere. However, because of the inability to move during the growth, plants suffer from various types of stress, including both abiotic and biotic stresses, which results from constantly changing surrounding environments. To overcome severe environmental conditions, plants have evolved an extremely complicated defense system against environmental stresses, which requires well-tuned interactions of various physiological processes, such as stress signal perception, transduction, gene expression, and biosynthesis of protective compounds. Plant hormone or phytohormones, a series of signal molecules that occur in generally low concentrations, have been identified and proven to play critical roles in these processes by triggering wide-range physiological responses. After intense studies for over one century, several phytohormones have been identified and their functions have been basically elucidated (Weijers *et al.*, 2018; Wang and Zhang, 2014;

Lymperopoulos *et al.*, 2018). Abscisic acid (ABA) is one of such phytohormones that has been shown to be the most important mediator in triggering responses to various abiotic stresses, such as drought, cold, osmotic and salt stresses (Zhu, 2002; Ma and Qin, 2014).

ABA, the stress hormone

The first isolation of ABA using cotton can be tracked back to the 1960s and ABA was shown to be able to stimulate leaf abscission and named accordingly (Ohkuma *et al.*, 1963). Through decades of research, the physiological functions of ABA in plants have been well studied, such as activation of stomatal closure to reduce transpiration, induction of seed dormancy and promotion of seed maturity (Schroeder *et al.*, 2001). When exposed to unfavorable environmental conditions, the cellular ABA level drastically increased, which in turn triggers stress response (Shinozaki and Yamaguchi-Shinozaki, 2007). Owing to advances of molecular techniques in genetics, proteomics and subcellular imaging in the past decades, understanding the signal perception pathway of ABA has been significantly progressed (Nishimura *et al.*, 2010). Besides, main enzymes and intermediary metabolites

involved in ABA metabolism have been identified mainly using the model plant *Arabidopsis*, which has provided us with an in-depth comprehension of this important hormone (Endo *et al.*, 2014; Ma and Qin, 2014).

Metabolism of ABA in higher plants

The biosynthesis of ABA originates from isopentenyl pyrophosphate (IPP), a common precursor in the biosynthesis of terpenes and terpenoids. In phytopathogenic fungi, IPP is first converted to farnesyl diphosphate and followed by a series of direct chemical modifications to generate active ABA (Inomata *et al.*, 2004), while higher plants hold a totally different route in which IPP is firstly converted to *trans*-β-carotene by multi-step reactions and further transformed to C_{40} carotenoid precursor, as the substrate of *de novo* synthesis. The synthesis of ABA starts in plastids from C_{40} carotenoid zeaxanthin, which is further converted to 9-*cis*-violaxanthin (or 9-*cis*-neolaxanthin) via the intermediate violaxanthin by the enzyme zeaxanthin epoxidase (ZEP) and a few yet unidentified isomerases. Nine-*cis*-violaxanthin is cleaved by 9-*cis*-epoxycarotenoid dioxygenase (NCED) to xanthoxin that is subsequently transported to the cytosol, where it is finally

converted to active ABA by the two enzymes, xanthoxin dehydrogenase and abscisic aldehyde oxidase (Nambara and Marion-Poll, 2005). At the onset of stress, cellular ABA levels increase to over a hundred times when compared with normal conditions, while deficiencies in the *de novo* synthesis result in extremely low ABA levels and hyper-sensitivity to drought stress (Urano *et al.*, 2009). These facts indicate the critical contribution of *de novo* synthesis to the stress tolerance of plants. However, although over-expression of ABA biosynthesis genes can result in enhanced stress resistance and higher survival under stress conditions, germination, growth and other normal physiological phenomena are inhibited due to the over-accumulation of ABA (Iuchi *et al.*, 2001; Han *et al.*, 2012). Therefore, maintenance of ABA homeostasis is important in plants, which requires precise balance between biosynthesis and catabolism.

The catabolism of ABA occurs mainly via two routes, degradation catalyzed by cytochrome P-450 type mono-oxygenases or conjugation to small molecules for inactivation. The key step of ABA degradation is the 8'-hydroxylation catalyzed by the CYP707A family, which affects aspects of both growth and stress responses (Okamoto *et al.*, 2006). The conjugation of ABA is mainly catalyzed by UDP-glucosyltransferase (UGT) to form ABA-

glucose ester (ABA-GE), which shows little activity as phytohormone and is considered to contribute to the rapid inactivation, long-distance transportation or simply utilized as storage (Priest *et al.*, 2006). ABA-GE can be hydrolyzed by specific isoenzymes of β-glucosidases, such as BGLU18 (also known as BG1) or BGLU33 (BG2) (Lee *et al.*, 2006; Xu *et al.*, 2012).

Regulation of ABA production under stress conditions

Stress-induced ABA production occurs mainly via two routes in *Arabidopsis*: a multi-step *de novo* synthesis as described above, and one-step hydrolysis from its inactive glucoside ABA-GE (Endo *et al.*, 2014; Lee *et al.*, 2006) and key enzymes for both routes have been identified (Figure 1). Several studies have shown that NCED play a central role as the rate-limiting enzyme in the *de novo* synthesis in response to stress, and the gene expression is induced by various abiotic stresses (Iuchi *et al.*, 2000; Thompson *et al.*, 2000). The *NCED* expression is also activated by ABA, suggesting that a positive-feedback regulation is operative in ABA biosynthesis (Xiong *et al.*, 2002). Another route of ABA production, the hydrolysis of ABA-GE, is catalyzed by BGLU18

and BGLU33, which are localized to the endoplasmic reticulum (ER) and vacuoles, respectively (Lee *et al.*, 2006; Xu *et al.*, 2012). It is considered that BGLU18 plays more crucial roles in stress-induced ABA production, since the loss of BGLU18 caused more severe stress-sensitive phenotypes in Arabidopsis compared with BGLU33-deficient mutants. Both BGLU18 and BGLU33 require to form high molecular weight polymers post-translationally to exhibit high enzyme activity. BGLU18-mediated ABA production is also considered to participate in periodicity in relation to circadian rhythm (Lee *et al.*, 2006), or the modification of stress-related root formation (Ondzighi-Assoume *et al.*, 2016), which might suggest that BGLU18 is responsible for the demands of rapid ABA production. However, the regulatory process of BGLU18 activation still remains elusive.

Previous studies have revealed that allantoin, an intermediate metabolite in purine catabolism, is able to enhance stress resistance in *Arabidopsis* by priming stress responses that are mediated by ABA and jasmonic acid (Watanabe *et al.*, 2014b; Takagi *et al.*, 2016). Allantoin leads to an increase in the basal ABA levels by promoting BGLU18 polymerization which is known as a molecular process to activate this enzyme. An interesting fact is that under stress, allantoin most probably accumulates in the ER (Werner and

Witte, 2011), where BGLU18 is also localized. These facts raise the possibility that the physiological processes associated with the ER are involved in the activation of BGLU18.

ER body, a unique defense strategy in the order Brassicales

The ER is a highly complicated network structure that is involved in a number of cellular functions, such as cellular signaling, diverse metabolic processes, biosynthesis, storage and transportation of proteins, and so on. In higher plants, the ER forms several different types of derivative compartments, such as precursor accumulating vesicles, KDEL-vesicles and ER bodies, all of which serve as repositories of ER-synthesized proteins and are considered to fulfill certain physiological functions related to its protein contents (Hara-Nishimura *et al.*, 1998; Toyooka *et al.*, 2000; Matsushima *et al.*, 2003a). Of particular interest is ER body, a unique structure that is reported only in the order *Brassicales,* which is so far considered to be involved in the responses to biotic stress (see below).

Originally reported in *Arabidopsis*, ER bodies are a unique spindle-shaped structure with a length of 5~10 μm and a width of 1 μm, which is localized into the epidermal cells around vascular

tissues in the leaves and roots (Matsushima *et al.*, 2002; Nakazaki *et al.*, 2019). In roots, ER bodies accumulate large amounts of PYK10 (BGLU23), a β-glucosidase that possesses myrosinase activity and is considered to play important roles in plant defense against biotic stress (Matsushima *et al.*, 2003a; Nakano *et al.*, 2017). Another research using radish (*Raphanus sativus*), a plant in *Brassicales* order, revealed that methyl jasmonate (MeJA), a key phytohormone in biotic stress responses, causes changes in the morphology and number of ER bodies with the accumulation of PYK10-like proteins (Gotté *et al.*, 2015). Due to its contents and inducibility by MeJA, physiological roles of ER bodies in roots is considered to serve for defense against biotic stress such as predators or pathogen attacks.

ER bodies in shoots are predicted to accomplish the similar function as in roots, since ER bodies in the cotyledons are known to mainly accumulate PYK10 and the formation of ER bodies is induced by mechanical wounding or treatment with MeJA (Matsushima *et al.*, 2002). However, a recent study found that specific cells of the leaf blades contained ER bodies whose main component was BGLU18, a shoot specific protein that is tightly related to stress-induced ABA production (Ogasawara *et al.*, 2009; Nakazaki *et al.*, 2019). These findings raise the possibility that ER

bodies in shoots may also be involved in abiotic stress responses, since shoots are considered to be a main part of stress-induced ABA production (Holbrook *et al*., 2002; Christmann *et al.*, 2007).

The aim of this study

The purpose of this study is to elucidate the mechanism of BGLU18 activation in rapid ABA production from ABA-GE, particularly in relation to the behavior of ER bodies in abiotic stress responses, using the model plant *Arabidopsis thaliana*.

In CHAPTER I, I conducted the experiments to determine the localization of BGLU18 at tissue and subcellular levels of rosette leaves, by subcellular fractionations followed by immunoblotting analysis and by microscopic observations of monomeric red fluorescence protein (mRFP)-tagged BGLU18 protein and GFP-marked ER/ER bodies.

In CHAPTER II, I investigated the involvement of ER bodies in abiotic stress responses leading to ABA production. To address this, I used transgenic plants expressing ER-localized GFP for the observation of ER bodies, and investigated the behavior of ER bodies in response to drought-induced dehydration, hyper-osmosis, and salt stresses, by analyzing their changes in number and

morphology. Arabidopsis *aln* mutants (deficient in allantoinase: ALN) were also used for the analysis to elucidate the relationship between ER bodies and BGLU18 activation, since BGLU18 is constitutively activated in the mutants due to constitutive accumulation of allantoin.

In CHAPTER III, I investigated the causal relationship between dynamic changes in ER bodies and activation of BGLU18 under abiotic stress. I examined the distributional changes in the ER network of BGLU18, along with the ABA-GE hydrolysis activity and ABA levels in the leaves. I also used an ER body-deficient mutant *nai2-2,* in order to further address the relation between ER-body function and BGLU18 activation. Finally, I monitored changes in foliar ABA levels in WT and ABA-metabolism mutants to investigate the contribution of BGLU18 to ABA production during an early phase of the stress response.

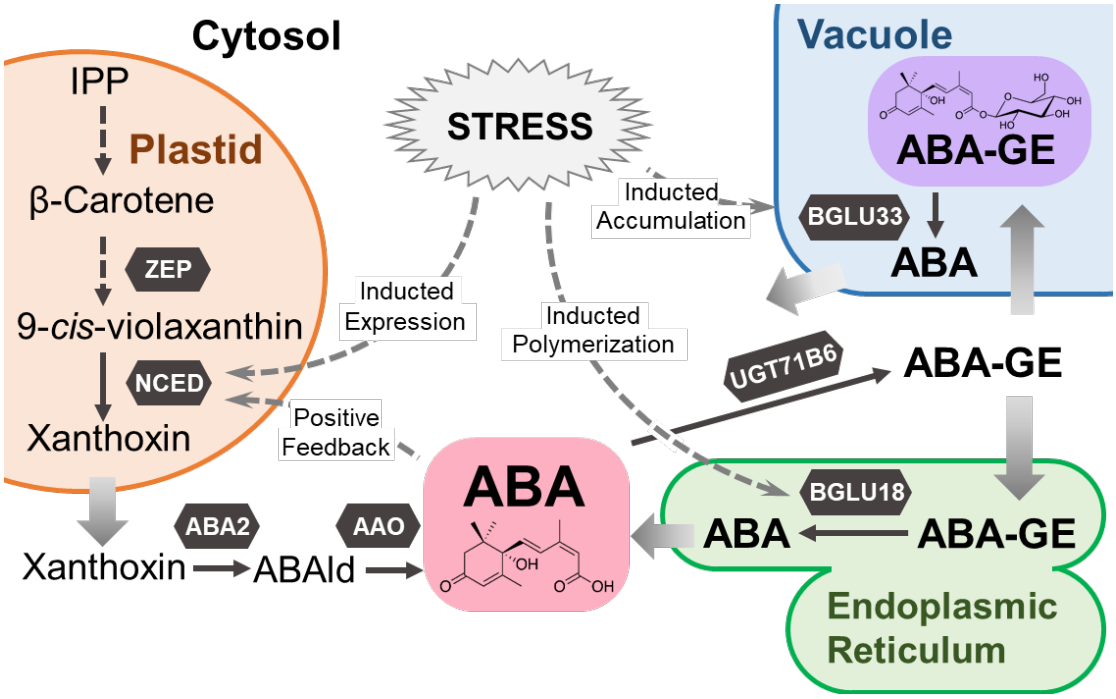

Figure 1. Overview of stress-induced ABA production
The two metabolic routes leading to ABA production, *de novo* synthesis and ABA-GE hydrolysis, are schematically illustrated with main metabolites and enzymes that are shown in hexagons. Abbreviations: IPP, isopentenyl pyrophosphate; ZEP, zeaxanthin epoxidase; NCED, nine-*cis*-epoxycarotenoid dioxygenase; ABA2, xanthoxin dehydrogenase; ABAld, abscisic aldehyde; ABA, abscisic acid; AAO, abscisic aldehyde oxidase; ABA-GE, ABA-glucose ester; BGLU33, β-glucosidase 33; BGLU18, β-glucosidase 18; UGT71B6, UDP-glucosyltransferase.

CHAPTER I

Leaf tissue distribution and subcellular localization of Arabidopsis BGLU18, a β-glucosidase responsible for stress-induced ABA production

Introduction

ABA is a chief plant regulator that acts mainly against abiotic stress, initiating stress signaling and directing downstream stress responses (Zeevaart and Creelman, 1988; Zhu, 2002). When plants are exposed to unfavorable environmental conditions such as drought, cellular ABA levels increase rapidly, inducing a wide array of physiological responses to protect plants from water loss and damage (Schroeder *et al*., 2001; Shinozaki and Yamaguchi-Shinozaki, 2007). Stress-induced ABA production occurs mainly via two routes in *Arabidopsis*: a multi-step *de novo* synthesis and a one-step hydrolysis from its inactive glucoside ABA-GE (Endo *et al*., 2014; Lee *et al*., 2006).

Although ABA-GE was long regarded as a simple byproduct of ABA catabolism, recent reverse-genetic studies have revealed that it constitutes an inactive pool of ABA that serves as an

alternative source of ABA production during physiological responses to environmental stimuli and stresses (Lee *et al*., 2006; Xu *et al*., 2012; Li *et al*., 2013; Watanabe *et al*., 2014b; Ondzighi-Assoume *et al*., 2016). In Arabidopsis, ABA-GE is hydrolyzed to release free ABA via a single-step reaction catalyzed by two β-glucosidase isoforms known as BG1 or BGLU18 (Lee *et al*., 2006) and BG2 or BGLU33 (Xu *et al*., 2012). BGLU18 is reportedly localized to the ER, whereas BGLU33 is a vacuolar enzyme. The loss of function *bg1* and *bg2* mutants exhibit enhanced sensitivity to drought and salt stress, and the *bg1 bg2* double mutants show additive effects. Conversely, overexpressing either enzyme alone confers significant salt tolerance in Arabidopsis. It is thought that ABA-GE hydrolysis contributes to rapid and local ABA release upon the onset of stress.

In this study, I focus on BGLU18 because this isoform probably plays more critical roles than BGLU33 with respect to ABA homeostasis and stress responses, based on the comparison of knock-out phenotypes of the two mutants (Lee *et al*., 2006; Xu *et al*., 2012). In order to know the physiological function of enzymes and its regulatory mechanism, it is important to understand tissue and subcellular localization of a given organ precisely. However, such information on BGLU18 in the leaves is still fragmental and

hardly comprehensive up to now, because of the reasons described below.

First, as mentioned earlier, BGLU18 was reported to be ER-localized. However, this result was obtained in transient expression assays using leaf mesophyll protoplasts. So, the subcellular localization of the native enzyme still remains to be demonstrated. Moreover, it is not known whether mesophyll tissues are the main site of BGLU18 distribution in leaves. Second, BGLU18 also occurs as a major component of ER body, but not the ER, which is formed only in the cotyledons upon mechanical wounding (Ogasawara *et al*., 2009). Although ER bodies induced in wounded cotyledons are suggested to play a role in defense against biotic stress, its relation to ABA metabolism is totally unknown. Finally, a recent report showed that in BGLU18 is localized to ER bodies that occur in only specific epidermal cells of leaf blades (Nakazaki *et al.*, 2019). This finding suggests the needs for a further detailed investigation because the above-ground tissues (mainly leaves) is the main part of stress-induced ABA production, at least in Arabidopsis and tomato plants (Holbroock *et al.*, 2002; Christmann *et al.*, 2007).

In this chapter, I conducted comprehensive examination of the tissue distribution and subcellular localization of native BGLU18 proteins in Arabidopsis leaves, by combining subcellular fractionation and immuno-

blotting analysis after the rosette leaves were separated into the blades and petioles. To confirm the results obtained, I further performed microscopic observations of the fluorescence-tagged BGLU18 that was transgenically expressed in Arabidopsis leaves as a fusion protein with mRFP.

Material and methods

Plant materials and growth conditions

Arabidopsis [*A. thaliana* (L.) Heynh.] accession Columbia-0 (Col-0) was used as wild type (WT) and all mutant lines used in this work were in the Col-0 background. Two transgenic lines, *GFP-h* and *GFP-h nai2-2*, which express green fluorescent protein (GFP) with an ER-retention signal, HDEL (GFP-h), in the WT and *nai2-2* backgrounds, respectively, were described by Hayashi *et al*. (2001) and Yamada *et al*. (2008). These *GFP-h* lines were crossed with some of the abovementioned mutants to allow ER/ER bodies to be visualized in each genetic background. To identify homozygous T-DNA insertion lines, I performed PCR based genotyping of each mutant using a gene-specific primer as shown in TABLE I.

Surface-sterilized seeds from WT and transgenic plants were sown on 0.3% (w/v) gellan gum plates of standard medium consisting of half-strength Murashige-Skoog basal salts and 1% (w/v) sucrose. After incubation at 4 °C, for 2 d, the plates were placed in a growth cabinet at 22 °C under 60–70 μmol photons m^{-2} s^{-1} of light with a 16-h photoperiod provided by white fluorescent lamps, and 14- or 16-day-old plants were used for all experiments.

Protein extraction and immunoblotting

Rosette leaves from 14-day-old plants were divided into leaf blades and petioles. Each leaf part was homogenized in 50 mM sodium phosphate buffer (pH 7.0) containing 150 mM NaCl, 0.02% (w/v) NaN_3, 10 mM dithiothreitol, and 0.1% (v/v) Triton X-100. An aliquot of the resulting protein extract was separated by sodium dodecyl sulfate-polyacrylamide gel electrophoresis (SDS-PAGE) using a 10% SDS gel and transferred onto a polyvinylidene difluoride membrane (Immobilon-P; Millipore, Billerica, MA, USA). After blocking with 3% (w/v) fat-free skim milk, the blotted membrane was incubated with primary antibodies anti-BGLU18 (Ogasawara *et al*., 2009), anti-NAI2 (Yamada *et al*., 2008), and anti-BINDING PROTEIN (BiP; Yamada *et al*., 2008) (each at 1:5000 dilution) and anti-GFP antibody (Abcam, Tokyo, Japan) (at 1:10,000 dilution). The membrane was incubated with anti-rabbit IgG secondary antibodies conjugated to horseradish peroxidase at 1:20,000 dilution. Chemiluminescent immunoblotting was performed using a Western Lighting Plus-ECL kit (Perkin-Elmer Life Sciences, Wellesley, MA, USA), and the signals were digitally captured on a VersaDoc 5000 imaging system using Quantity One software (Bio-Rad Laboratories, Hercules, CA, USA) and analyzed using ImageJ software (National Institute of Health, Bethesda, MD, USA) to determine the relative

intensities of the protein bands.

Subcellular fractionation

The fractionation scheme followed that of Matsushima *et al.* (2003) with slight modifications. Shoots of 16-day-old plants were cut on ice with a razor blade and homogenized in three volumes (v/w) of ice-cold chopping buffer containing 50 mM HEPES-NaOH (pH 7.5), 5 mM EDTA, 0.4 M sucrose, and SIGMAFAST Protease Inhibitor Tablets (one tablet per 50 mL; Sigma-Aldrich, St. Louis, MO, USA). The homogenate was passed through four layers of gauze, and the resulting filtrate (designated as the total extract) was separated into four fractions by differential centrifugation as follows. The total extract (1 mL) was centrifuged at 1000 *g* for 20 min and the pellet was saved as the P1 fraction. The supernatant was re-centrifuged at 8000 *g* for 20 min to separate the pellet (P8 fraction) from the supernatant, which was subjected to ultra-centrifugation at 100,000 *g* for 60 min to obtain the microsomal pellet and soluble supernatant (P100 and S100 fractions, respectively). All centrifugation was performed at 4 °C. Each pellet was resuspended in 500 μL chopping buffer, and the fractions were loaded on a volume-to-volume basis (30 μL) onto an SDS-PAGE gel for immunoblotting.

Transient expression assays

A fusion gene between *BGLU18* and *mRFP* was constructed based on its *GFP* counterpart as described in Lee *et al*. (2006). DNA sequences encoding the signal peptide region (amino acid residues 1–39) and mature polypeptide region (residues 40–528) of BGLU18 were separately PCR-amplified from the corresponding cDNA (pda05953; provided by RIKEN BioResource Center, Tsukuba, Japan) and translationally fused to the 5' and 3' ends, respectively, of the coding sequence of mRFP (Figure I-1; for primers, see Table I). The resulting chimeric *mRFP-BGLU18* gene was cloned into the pENTR vector (Thermo Fisher Scientific, San Jose, CA, USA) and, after sequence verification, transferred into pUGW2 (Nakagawa *et al*., 2007) driven by the *Cauliflower mosaic virus 35S RNA* promoter. The resulting plasmid was introduced into leaf petioles of 14-day-old *GFP-h* plants by particle bombardment (PDU-1000/He, Bio-Rad Laboratories). The bombarded samples were incubated at 22°C in the dark for 18 h and analyzed by confocal laser-scanning fluorescence microscopy (Fluoview FV1000D; Olympus, Tokyo, Japan). GFP and mRFP fluorescence were detected at 485–535 and 585–650 nm, respectively, following excitation with 473- or 559-nm diode lasers.

Results

BGLU18 is abundant in leaf petioles and is predominantly localized to ER bodies

BGLU18 mRNA is expressed at high levels in the aerial parts of plants, particularly vegetative leaves (Xu *et al*., 2004; Lee *et al*., 2006); this finding is supported by publicly available microarray data from the Arabidopsis eFP Browser (Figure I-2; Winter *et al*., 2007). However, few studies have examined the protein level of BGLU18, except for an experiment in which a *BGLU18* transgene was ectopically expressed in transgenic Arabidopsis under a strong constitutive promoter (Lee *et al*., 2006). I examined the distribution of BGLU18 in the aboveground tissues (mostly leaf blades and petioles) of 14-day-old Arabidopsis plants grown under normal conditions. Immunoblotting analysis detected more BGLU18 in petioles than in leaf blades (Figure I-4A), which is consistent with the quantitative expression data (Figure I-3).

To assess the subcellular localization of BGLU18, I performed subcellular fractionation and immunoblotting using leaf tissues from *GFP-h* plants that stably produced GFP with an ER-retention signal (Hayashi *et al*., 2001). BGLU18 protein is mainly detected in the P1 and P8 fractions, which were enriched for ER bodies, as well as small

amounts in the microsomal P100 fraction (where, as expected, GFP-h was most abundant), but not in the soluble S100 fraction (Figure I-4B). The BGLU18 levels in the fractionated samples were intermediate between those of the canonical ER-body-specific protein NAI2 and the major ER-lumen protein BiP. To obtain independent evidence for this localization pattern, I transiently expressed an *mRFP-BGLU18* translational fusion construct in the petiole tissues of *GFP-h* plants. In the transformed plants, most mRFP signals overlapped with those of GFP, representing ER and ER bodies (Figure I-4C). Therefore, both of these approaches demonstrated that under normal conditions, BGLU18 primarily occurs as a component of ER bodies and to a minor extent in the ER in leaf petioles.

Previously unrecognized ER bodies occur in the leaf petioles

Interestingly, before the transient expression experiments, I already observed numerous spindle-shaped GFP spots in the leaf petiole and some in the leaf blade (more in the midrib and edge and fewer in the lamina) of *GFP-h* plants in the WT background (Figure I-5A, B). These ER bodies were evenly distributed on the adaxial and abaxial sides of the leaf. The observations indicate that the formation of these structures was not induced by bombardment but rather existed constitutively. By

contrast, few GFP spots were detected in *GFP-h nai2-2* plants (Figure I-5C). Because *nai2* mutants lack constitutive ER bodies (Yamada *et al*., 2008), these observations indicate that substantial amounts of BGLU18 are localized to previously unrecognized, constitutive ER bodies that occur in the leaf petioles of Arabidopsis plants. The predominant distribution of BGLU18 in the leaf petiole suggests that this protein is physiologically important in this part of the leaf.

Discussion

To begin with this research, firstly, I addressed the tissue and subcellular localization of BGLU18 in Arabidopsis leaves. This was because the available information was not comprehensive. BGLU18 was originally reported to be localized to the ER of leaf protoplasts on the basis of a constitutive overexpression study (Lee *et al*., 2006). However, the enzyme was subsequently identified as a major component of ER bodies that were induced in wounded cotyledons (Ogasawara et al., 2009). Very recently, it was also found in a newly identified ER body that was constitutively present but limited to specific epidermal cells of leaf blades (Nakazaki *et al*., 2019). Here I showed that this enzyme occurred more abundantly in leaf petioles than in leaf blades (Figure I-4A), which is consistent with the distribution pattern of ER bodies in shoots (Figure I-5). The data are also supported by BGLU18 transcript expression which is the highest in the petioles (Figure I-3). Moreover, I found that at the subcellular level, BGLU18 was predominantly, but not exclusively, localized to the ER bodies of the epidermal cells (Figure I-4BC), which is different from the previous finding reporting the ER localization (Lee *et al*., 2006). The discrepancy can be explained by that Lee *et al*. (2006) used mesophyll protoplasts to determine the

subcellular localization of BGLU18 in transient expression assays: however, it is unlikely that leaf mesophylls are the main part of BGLU18 protein distribution as demonstrated by immunoblotting (Figure I-4A) and little ER bodies were observed there (Figure I-5). Overall, the results obtained here thus substantially complemented the previous findings regarding BGLU18, by demonstrating the protein's major tissue location in the leaves and confirming its presence in both the ER and ER bodies. In addition, the current findings, together with those of Nakazaki et al. (2019), establish that ER bodies are constitutively present in true leaves of Arabidopsis plants, even though it was previously thought that they rarely occur in healthy rosette leaves (Matsushima et al., 2002; Nakano et al., 2014).

ER bodies have been implicated in resistance to biotic stress such as pathogenic microbial infection and insect herbivory/wounding (Sherameti *et al*., 2008; Yamada *et al*., 2011; Nakano *et al*., 2017; Nakazaki *et al*., 2019). The results here may extend the physiological role of ER bodies to abiotic stress defense, thanks to the known role of BGLU18 in ABA metabolism and homeostasis (Lee *et al*., 2006; Watanabe *et al*., 2014b). It is possible that ER bodies participates in the regulation process of BGLU18 activation or stress responses and petiole is a main part of stress-induced ABA production in shoots. Therefore, I examine these possibilities in the following chapters.

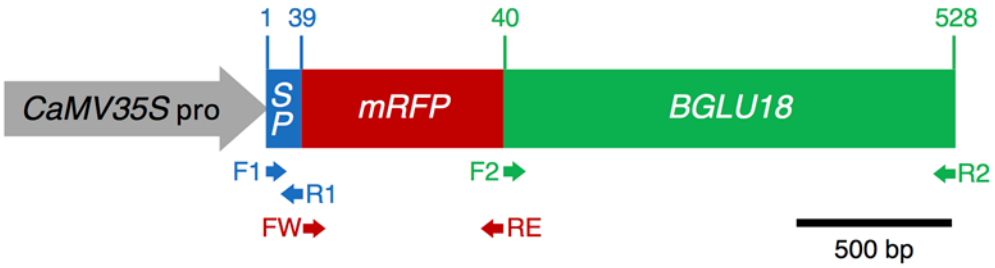

Figure I-1. Construction of the *mRFP-BGLU18* fusion plasmid. Coding sequences for the NH_2-terminal region containing a putative signal peptide (SP; residues 1–39) and the mature polypeptide region (residues 40–528) of BGLU18 were individually obtained by PCR using the full-length cDNA clone (GenBank: AY056415) and translationally fused to 5' and 3' ends, respectively, of the *mRFP* gene under the control of the *CaMV35S* promoter in pUGW2 (Nakagawa *et al*., 2007). Arrows denote PCR primers used for constructing the plasmid and primer sequences are shown in TABLE I. *CaMV35S* pro, Cauliflower mosaic virus 35S promoter; SP, signal peptide from BGLU18; mRFP, monomeric red fluorescence protein; BGLU18, mature polypeptide of BGLU18.

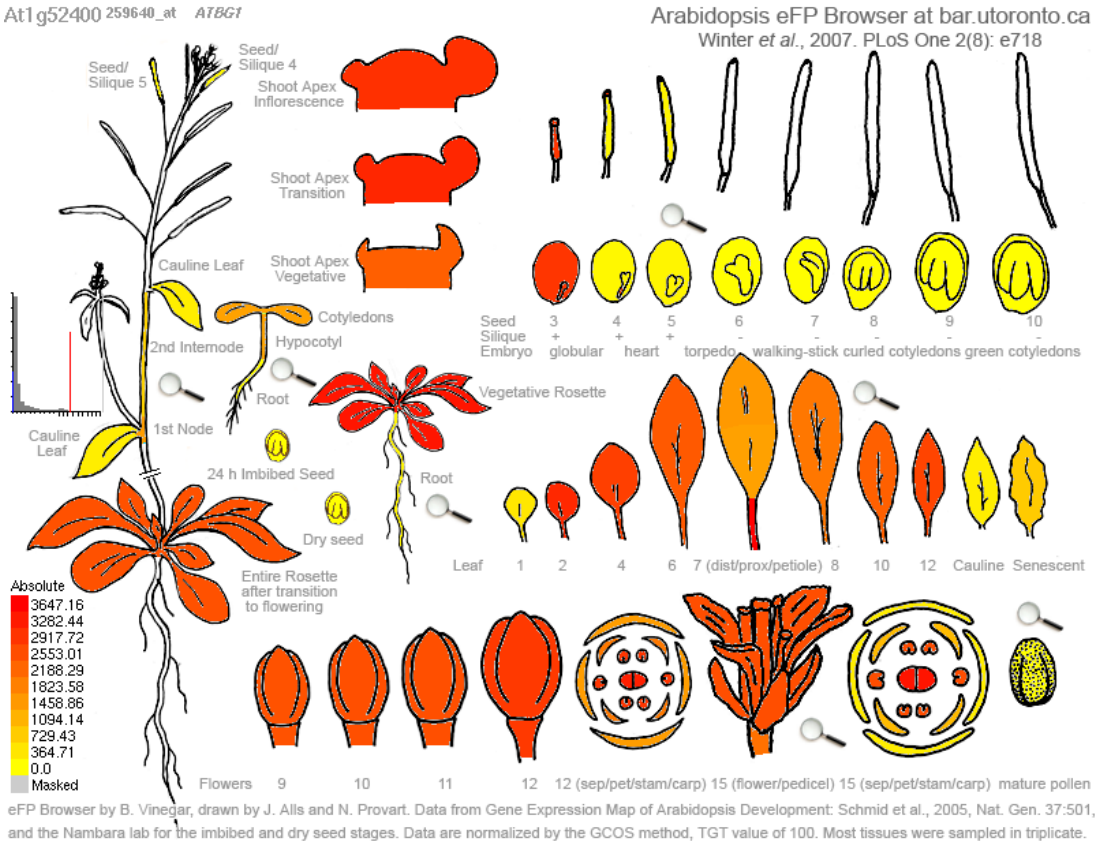

Figure I-2. Expression profile of the *BG1*/*BGLU18* gene (At1g52400) in different tissues of growing Arabidopsis plants. Obtained from the Arabidopsis eFP browser web server (http://bar.utoronto.ca/efp/cgi-bin/efpWeb.cgi) and reprinted from Winter *et al.* (2007).

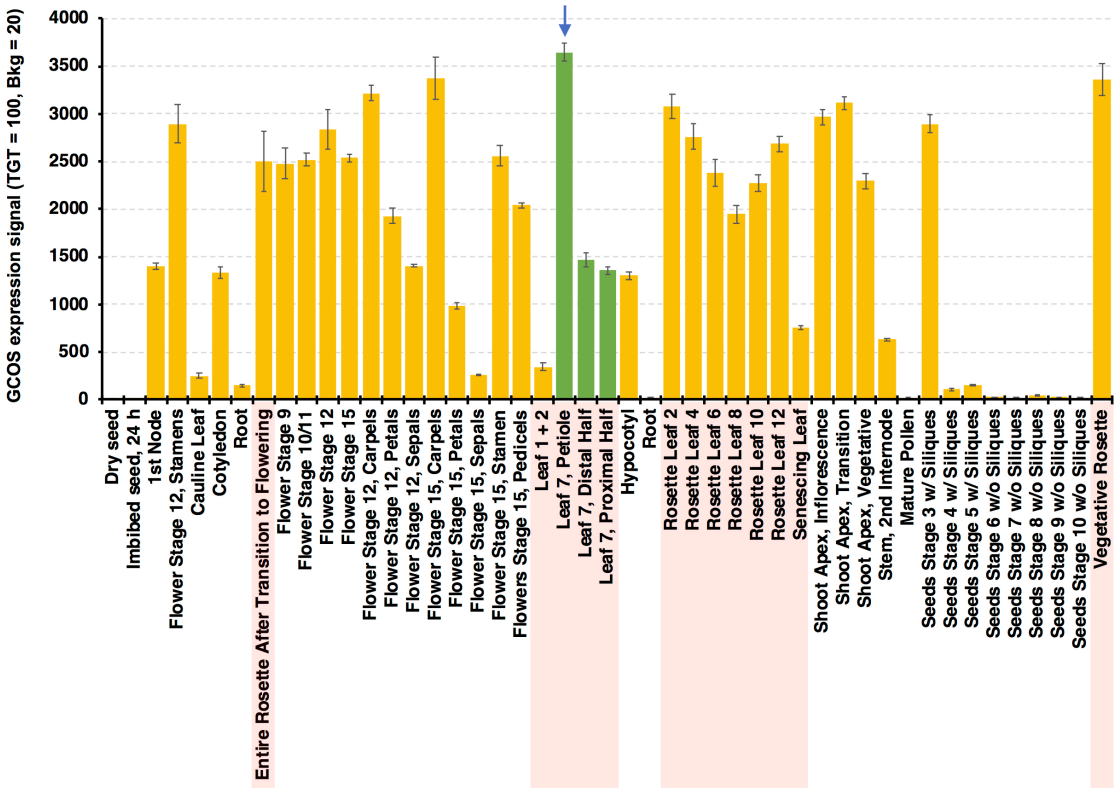

Figure I-3. Quantitative comparison of *BG1*/*BGLU18* (At1g52400) expression in different tissues of growing Arabidopsis plants. Expression signal values (mean ± SD) were obtained from the Arabidopsis eFP browser web server (http://bar.utoronto.ca/efp/cgi-bin/efpWeb.cgi). Rosette leaf samples are indicated by the pink background color. The expression data of three different parts (petiole, proximal blade, and distal blade) from a single leaf (rosette leaf 7) are shown in green bars where the expression in the leaf petiole is indicated by the blue vertical arrow.

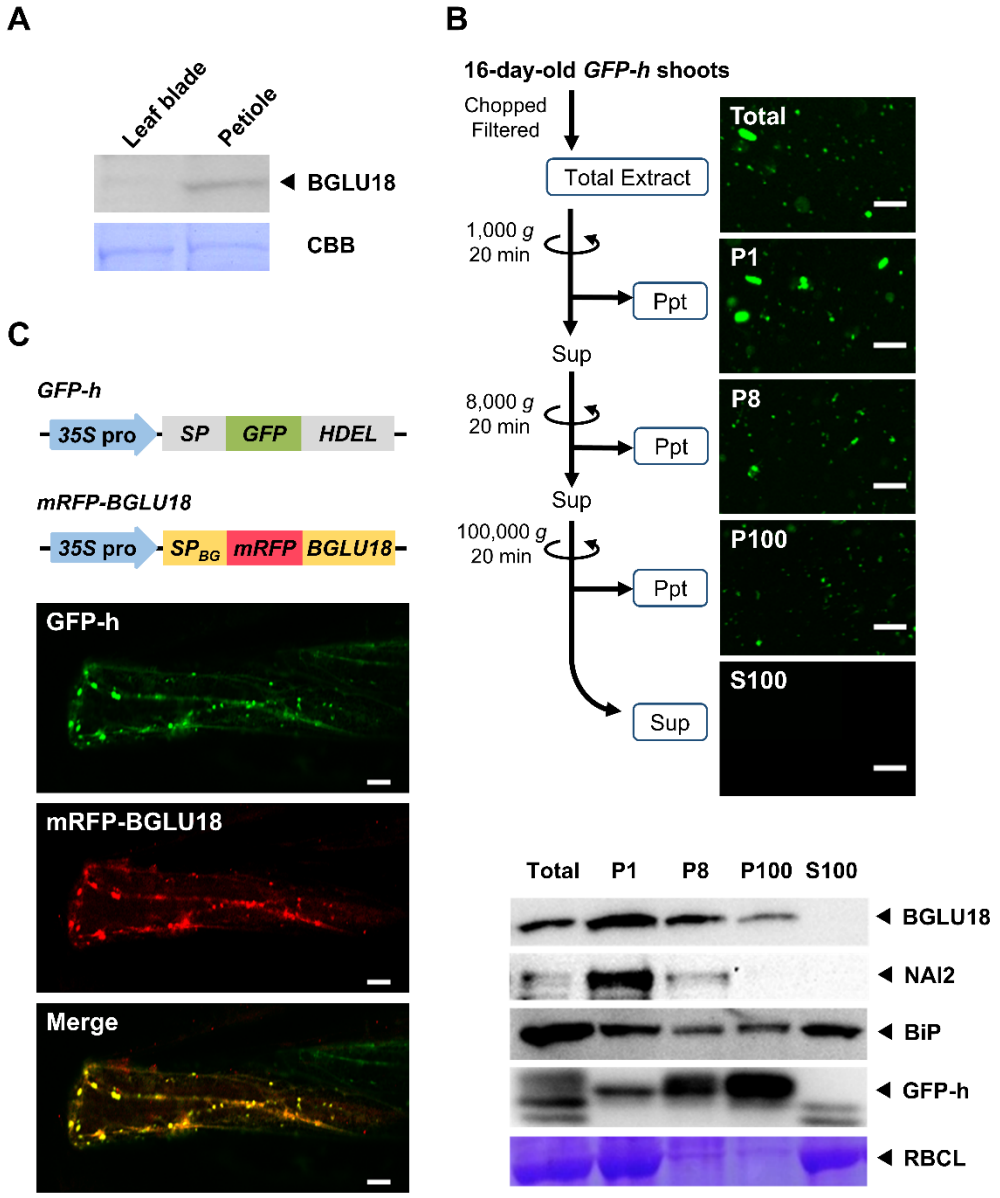

Figure I-4. Tissue distribution and subcellular localization of BGLU18 in Arabidopsis leaves. (A) Tissue distribution within true leaves. Immunoblotting analysis was performed with anti BGLU18 antibodies using 30 μg of total protein extracted from leaf blades and petioles of 14-day-old plants grown under normal conditions. (B) Subcellular distribution of BGLU18 as determined by biochemical fractionation. The upper panel shows the fractionation scheme and typical fluorescence images of subcellular fractions prepared from shoot extracts of GFP-h plants. P1, P8, and P100 denote pellets (Ppt) obtained after centrifugation at 1000, 8000, and 100,000 *g*, respectively, and S100 is the supernatant (Sup) after centrifugation at 100,000 *g*. Scale bars = 20 μm. The lower panel shows typical immunoblotting results for the distribution of BGLU18, NAI2, BiP, and GFP-h in the subcellular fractions. The large subunits of RBC (RBCL) was stained with CBB. Analyses were conducted on a volume to volume basis.

(**Figure I-4** legend continued)
(C) Subcellular localization of the fusion protein mRFP-BGLU18 as determined by confocal laser scanning fluorescence microscopy. Above, GFP and mRFP fusion constructs used for visualizing ER/ER bodies and BGLU18, respectively. *35S* pro, Cauliflower mosaic virus 35S promoter; SP, signal peptide from pumpkin 2S albumin; GFP, green fluorescence protein; HDEL, ER retention signal; SPBG, signal peptide from BGLU18; mRFP, monomeric red fluorescence protein; BGLU18, mature polypeptide of BGLU18. Below, representative fluorescence images of leaf petiole epidermal cells of a GFP-h plant transiently expressing BGLU18-mRFP by particle bombardment. Scale bars = 20 μm. All the experiments were repeated three times to confirm the reproducibility of the results, and one representative result is shown for each.

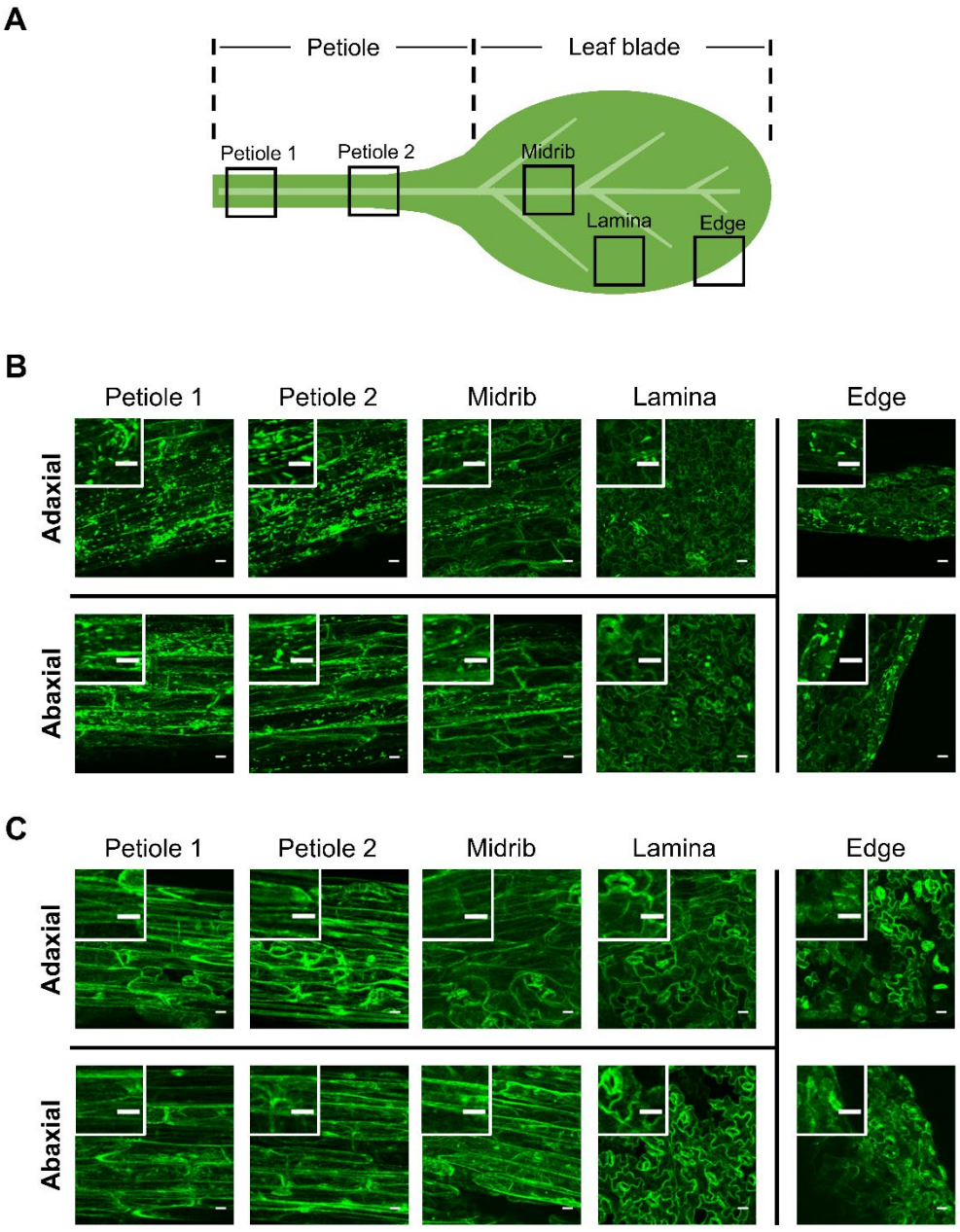

Figure I-5. Tissue distribution of ER bodies in Arabidopsis leaves. The first true leaf from a 14-day-old normally grown plant was used. (A) Leaf portions subjected to fluorescence microscopic observation for GFP. (B and C) Representative fluorescence images of different leaf portions from *GFP-h* (B) and *GFP-h nai2-2* plants (C), with enlarged images in insets. Scale bars = 20 μm.

Table I. Primers used for making an mRFP-BGLU18 fusion protein construct.

AGI[a]	Gene symbol[b]	Direction	Sequence (Designation)	Use
At1g52400	*BG1*/*BGLU18*	Forward	5′-CACCATGGTGAGGTTCGAGAAGGTT-3′ (F1)	*mRFP-BGLU18* fusion construction (for signal peptide)
		Reverse	5′-AAATTTGTCAGGCAGGCCTGCACC-3′ (R1)	*mRFP-BGLU18* fusion construction (for signal peptide)
		Forward	5′-AGCAGATTAAACTTCCCTGAAGGC-3′ (F2)	*mRFP-BGLU18* fusion construction (for mature polypeptide)
		Reverse	5′-CTAGAGTTCTTCCCTCAGCTTGG-3′ (R2)	*mRFP-BGLU18* fusion construction (for mature polypeptide)
–	*mRFP*	Forward	5′-ATGGCCTCCTCCGAGGACGTCATCA-3′ (FW)	*mRFP-BGLU18* fusion construction
		Reverse	5′-GGCGCCGGTGGAGTGG-3′ (RE)	*mRFP-BGLU18* fusion construction

[a] *Arabidopsis thaliana* gene identifier (AGI) code assigned according to the guidelines for nomenclature used for Arabidopsis genes (https://www.arabidopsis.org/portals/nomenclature/guidelines.jsp).

[b] Gene symbol, as provided by The Arabidopsis Information Resource (TAIR; release 10; https://www.arabidopsis.org/), except for *mRFP*.

CHAPTER II

The possible involvement of dynamic changes in the endoplasmic reticulum in BGLU18 activation under stress

Introduction

Endoplasmic reticulum (ER) is an extremely complicated network structure that has critical functions notably in cellular signaling, and secretion and membrane transport of proteins. To fulfill its functions, special compartments are often developed from the ER and serve as repositories of ER-synthesized proteins. (Hara-Nishimura *et al.*, 1998; Toyooka *et al.*, 2000; Matsushima *et al.*, 2003a). One of such ER-derivatives is ER body that is unique to the *Brassicales* order including Arabidopsis, which has a unique spindle-shaped structure with a length of 5~10 μm and a width of 1 μm. It has been reported that ER bodies are localized in epidermal cells of roots, hypocotyls, cotyledons and true leaf blades, to varied extent (Matsushima *et al.*, 2002; Nakano *et al.*, 2014; Nakazaki *et al.*, 2019). Since ER bodies accumulate large amounts of β-glucosidases, such as PYK10 (BGLU23) which possesses

myrosinase activity, this unique organelle has been considered to play critical physiological roles in plant defense against biotic stress such as wounding caused by microbial infection or insect herbivory (Matsushima *et al.*, 2003a; Nakano *et al.*, 2017). However, in the previous chapter, I found that BGLU18, a key enzyme of ABA production, is localized to ER bodies in the petiole of true leaves, which suggests that ER bodies may also participate in abiotic stress responses.

Previous researches have shown that changes in number and morphology of ER bodies take place in response to biotic stress, which is considered to be involved in their function in the response to biotic stress (Matsushima *et al.*, 2002; Ogasawara *et al.*, 2009). In radish (*Raphanus sativus*), another species in *Brassicales* order, similar dynamic changes in ER bodies can also be observed when seedlings are treated by MeJA, a key hormone in biotic stress responses, with the accumulation of PYK10-like β-glucosidase proteins in ER bodies (Gotté *et al.*, 2015). However, it is totally unknown whether or not such dynamic changes in ER bodies are induced in response to abiotic stress, such as drought and salt stress.

Therefore, in this chapter, I investigated the effect of various abiotic stress, such as drought-induced dehydration, osmotic stress,

and high salinity, on the behavior of ER bodies in petiole tissues of Arabidopsis. Particularly, the response of petiole ER bodies to dehydration was examined in the details. I also examined the effect of allantoin on the ER bodies to know whether the behavior of ER bodies is somehow related to the modulation of BGLU18 activity, since allantoin is known to activate BGLU18 under non-stress conditions (Watanabe *et al.*, 2014b).

Material and methods

Plant materials and growth conditions

The plant materials and growth conditions are described as in CHAPTER I. The seeds of the following SALK T-DNA insertion lines were obtained from the Arabidopsis Biological Resource Center (Ohio State University): *allantoinase-1* (*aln-1*; SALK_000325; Watanabe *et al*., 2014*b*) for *ALLANTOINASE* (At4g04955), *bglu18* (SALK_075731C; Ogasawara *et al.*, 2009) for *BGLU18* (At1g52400), The *aln-1 bglu18* double mutant was described previously (Takagi *et al.*, 2016). These *GFP-h* lines were crossed with some of the abovementioned mutants to allow ER/ER bodies to be visualized in each genetic background. To identify homozygous T-DNA insertion lines, I performed PCR based genotyping of each mutant using a gene-specific primer as shown in Table II-1.

Protein extraction, SDS-PAGE and western blotting

Protein extraction, SDS-PAGE and western blotting were performed as described in CHAPTER I.

Transient expression assay

The transient assay by particle bombardment was carried out as described in CHAPTER I.

Stress treatments and relative water content (RWC) measurements

Stress treatments were applied to plants grown aseptically in Petri plates for 14 or 16 days. Drought-induced dehydration stress was induced by removing the lids from the plates for the indicated periods of time under aseptic conditions on a laminar flow hood (Nanjo *et al*., 1999). For osmotic stress, plants were transferred onto solid medium containing polyethylene glycol (PEG) (molecular weight 8000; Sigma-Aldrich) to impose a low water potential of approximately –0.5 MPa, followed by incubation for 12 h (Watanabe *et al*., 2014*b*). Salt stress was imposed by transferring the plants onto solid medium containing 150 mM NaCl and incubating them for 12 h. As a control, plants were transferred to standard medium containing no additives. After stress treatment, the plants were immediately subjected to further analysis or stored at –80 °C.

Leaf RWC was measured as described by Barrs and Weatherley (1962). Primary and secondary leaves were collected from at least ten plants and immediately weighed to determine fresh weight (FW), followed by rehydration by floating on water for 3 h to determine turgid weight (TW). Dry weight (DW) was recorded after drying these samples at 80 °C to a constant weight. RWC was calculated using the following formula: RWC = (FW – DW)/(TW – DW) × 100.

RNA extraction and reverse transcription-quantitative PCR (RT-qPCR)

RNA extraction and RT-qPCR were performed as described (Watanabe *et al*., 2014*b*). Briefly, total RNA was extracted from the aerial parts of plants using a NucleoSpin RNA kit (Macherey-Nagel GmbH & Co, Düren, Germany), and 1 μg of RNA was reverse-transcribed into cDNA using a ReverTra Ace qPCR RT kit (Toyobo, Osaka, Japan). qPCR was carried out with a KAPA SYBR FAST qPCR Kit (Kapa Biosystems, Inc., Woburn, MA, USA) in a 20 μL reaction containing 1× Master Mix, 0.2 μM forward and reverse primers, and 10 ng cDNA. The thermal cycling conditions were 95 °C for 3 min and 40 cycles of 95 °C for 15 s/65 °C for 40 s, followed by 65–95 °C melting curve analysis with 0.5 °C increments. The relative transcript levels of

target genes were calculated using the comparative C_T method (Livak and Schmittgen, 2001) after normalization to *SAND FAMILY PROTEIN* (*SAND*; At2g28390), *E2 UBIQUITIN-CONJUGATING ENZYME 9* (*UBC9*; At4g27960), or *PENTATRICOPEPTIDE REPEAT* (*PPR*; At1g62930) as a reference. The primer sequences for the target and reference genes are listed in Table II-1.

Microscopic observation and analysis of ER body number and size

ER bodies, as visualized by the expression of GFP-h (GFP with an ER-retention signal; Hayashi *et al*., 2001), were detected by fluorescence microscopy using the FV1000D system as described above. To estimate the number of ER bodies, confocal microscopic images of a petiole sample were acquired at a 2-μm interval from the first (surface) to 30th (inside) layer in *z*-stack direction (60 μm in depth), and the 30 images obtained were merged using Olympus Fluoview software. A merged *z*-stack typically contained 12 to 15 cells with GFP-visualized ER bodies. The areas of the individual cells were measured using ImageJ, and the number of ER bodies in each cell was counted manually.

For time-course analysis of ER-body number and size in dehydration-stressed plants, GFP fluorescence was observed in petiole samples under an LSM700 confocal laser-scanning

microscope (Carl Zeiss, Jena, Germany) using a 488-nm diode laser line and a 490–530 nm detection band. All images were taken using the same settings: laser output strength, 22%; magnification, 40-fold; resolution, 512 × 512 pixels/112.5 × 112.5 μm; pinhole, 100 μm; gain parameters, 550; and 12-bit coloring. The region of interest was selected manually as a window of 512 × 512 pixels, and fluorescence analysis was performed using ImageJ following the procedure of Nagano *et al*. (2009), with the threshold set from 40 to 255 for particle analysis.

ABA measurement

ABA was purified and quantified as described (Preston *et al.* 2009) with slight modifications. Plant tissues were frozen in liquid nitrogen and crushed using a steel-bead homogenizer (Tissue Lyser II; Qiagen, Hilden, Germany). The resulting powder was suspended and incubated for 1 h in extraction buffer (80% acetonitrile and 1% acetic acid, v/v, in ultrapure water) that included 3’, 5’, 5’, 7’, 7’, 7’-hexadeuterated ABA (d_6-ABA; Santa Cruz Biotechnology, Santa Cruz, CA, USA) as an internal control. A clear extract was obtained by centrifugation, and the residues were re-extracted with extraction buffer without d_6-ABA. Both extracts were combined

and pre-concentrated by solid phase extraction using Oasis HLB and MCX cartridges (1 cc/30 mg, 30 μm particle size; Waters Corporation, Milford, MA, USA) before being subjected to further purification and analysis by liquid chromatography-electrospray ionization-tandem mass spectrometry (LC-ESI-MS/MS).

Measurement of ABA-GE hydrolysis activity

ABA-GE hydrolysis activity in microsomal fractions (P100 as described above) was assayed as described previously (Watanabe *et al.*, 2014*b*). The pelleted microsomal fractions were resuspended in ice-cold buffer containing 25 mM HEPES (pH 7.0), 250 mM sucrose, 10 mM $MgCl_2$, 1 mM dithiothreitol, and 1% (v/v) Triton X-100, and aliquots of the sample were incubated in 100 nM ABA-GE (OlChemim Ltd., Olomouc, Czech Republic) at 37 °C for 1 h. The liberated ABA was recovered by solid-phase extraction and quantified by LC-ESI-MS/MS as described above.

Statistical analysis

Results are presented as means with standard deviations (SD) from at least three independent experiments, unless otherwise

noted. Statistical significance of differences between two groups was determined using unpaired Student's *t*-test after comparing the variances of the samples by *F*-test. Comparisons among three or more groups were performed using one-way analysis of variance (ANOVA) with Tukey's multiple comparison test. Linear regression analysis was applied to examine the correlation between RWC and time following stress treatment.

Results

ER bodies increase in number in response to abiotic stress and undergo dynamic changes during dehydration stress and recovery

Since BGLU18 is a key enzyme in ABA production and ABA plays pivotal roles in adaptive responses to abiotic stress, I investigated whether ER bodies in leaf petioles respond to abiotic stress by subjecting *GFP-h* plants to drought-induced dehydration stress, PEG-induced osmotic stress, and high salinity (Figure II-1). For dehydration treatment (up to 60 min), I monitored changes in the dehydration status of stressed plants by measuring leaf RWC and the transcript levels of three canonical stress-responsive genes, *RESPONSIVE TO DESICCATION 29A* (*RD29A*; At5g52310), *RD29B* (At5g52300), and *RD26* (At4g27410), along with *BGLU18*, which is also known to be induced by dehydration (Lee *et al*., 2006; Figure II-3). Leaf RWC decreased progressively (Figure II-1A), whereas the transcript levels of all genes except *BGLU18* significantly increased with increasing duration of dehydration stress (Figure II-1B; Figure II-2), thus supporting the validity of the stress treatment. Under dehydration treatment, the number of petiole ER bodies increased significantly (3.2-fold) compared to the unstressed controls (Figure II-1C). The number of ER bodies also increased significantly after 12-h

treatment with NaCl or PEG (1.5- to 1.7-fold). These results demonstrate that in the leaf petiole, ER bodies not only exist constitutively, but their formation is also induced by these abiotic stresses.

To examine the responses of leaf petiole ER bodies to abiotic stress in further detail, I monitored the changes in their number and size over the course of a 120-min dehydration treatment and following a period of recovery (Figure II-4). Compared to control conditions, the number of ER bodies began to increase significantly within 30 min after the onset of stress and nearly doubled at 60 min, after which it returned to the original level (90 min) and decreased further (120 min) (Figure II-4A, B). Coincident with the decline in the number of ER bodies, their average size was also reduced at 90 and 120 min (Figure II-4A, C). However, these ER bodies returned to their original state after recovery from dehydration, suggesting that the observed changes are part of the physiological response to stress treatment. These results demonstrate that the ER in the leaf petiole undergoes dynamic changes, as evidenced by the reversible changes in ER-body status, during dehydration stress and recovery.

The number of ER bodies increases in aln *mutants and in response to allantoin treatment, causing stress-independent BGLU18 activation, but the* bglu18 *mutation abrogates this increase*

To assess the relationship between BGLU18 and abiotic stress responses of leaf petiole ER bodies, I examined the status of ER bodies in the *aln-1* mutant, which accumulates allantoin, since this purine metabolite activates BGLU18 and increases basal ABA levels under normal conditions (Watanabe *et al.*, 2014b). In the *aln-1* mutant, like WT plants, BGLU18 predominantly localized to leaf petioles (Figure II-5A). Consistent with previous findings, ABA-GE hydrolysis activity was highest in *aln-1*, followed by WT, and lowest in *bglu18*, which I used as a background control given that BGLU18 is a member of a large enzyme family (47 members in Arabidopsis; Xu *et al*., 2004; Nakano *et al*., 2014) (Figure II-5B). I crossed *aln-1* with the *GFP-h* line to visualize ER and ER bodies. In the absence of stress, the resulting *GFP-h aln-1* plants had a significantly (3.8-fold) more ER bodies in petiole tissues than *GFP-h* plants (Figure II-5C). Treating the parental *GFP-h* plants with exogenous allantoin (100 μM) resulted in a similar increase in the number of ER bodies, confirming the notion that allantoin increases the abundance of ER bodies. However, introducing the *bglu18* mutation into the *GFP-h aln-1* mutant background (*GFP-h aln-1 bglu18*) decreased ER body number to normal levels, as observed in *GFP-h* and *GFP-h bglu18* plants (Figure II-5D). These findings suggest that BGLU18 is a necessary component in the induction of ER body formation in the leaf petiole. This

idea is supported by the observation that transient expression of *mRFP-BGLU18* in the *GFP-h aln-1* mutant resulted in strong RFP fluorescence on ER bodies (Figure II-5E). Collectively, these results uncover a direct relationship between ER-body number and BGLU18-mediated ABA-GE hydrolysis activity.

Discussion

Considering the known role of BGLU18 in ABA metabolism and its predominant localization in ER bodies which was shown in the preceding chapter, in this chapter, I investigated whether ER bodies in the leaves respond to abiotic stress conditions, which had not been examined previously. In a pattern similar to the wounding response, the number of ER bodies in leaf petioles increased significantly in response to drought-induced dehydration stress, osmotic stress, or high salinity (Figure II-1). Thus, dynamic changes in ER-body status constitute a general stress response in Arabidopsis. Nevertheless, the changes in leaf petioles occurred over a much shorter period (30–60 min for dehydration and 12 h for osmotic and salt stress; Figures II-1 and II-4) than the time required for wounding responses in leaf blades (44–66 h; Matsushima *et al.*, 2002). In addition, the dehydration response of ER bodies in stressed cells was reversed following the removal of stress (Figure II-4), whereas the wounding response involving ER bodies requires cellular destruction to exert a so-called “mustard oil bomb” strategy, producing secondary metabolites toxic to potential pathogens and herbivores (Yamada *et al.*, 2011; Nakano *et al*., 2017). These differences might reflect the distinct roles played by

ER bodies whose formation is induced upon dehydration and wounding, that is, in abiotic versus biotic stress responses.

Given our observations in leaf petiole tissues, I was interested in exploring whether abiotic-stress-induced dynamic changes in ER-body status were physiologically relevant to BGLU18 function. For this, I examined the effect of allantoin on ER-body dynamics, as this ER-related purine metabolite can activate BGLU18 and enhance basal ABA levels, while the inability to produce allantoin results in hypersensitivity to dehydration in Arabidopsis (Watanabe *et al.*, 2010, 2014a, b). Both endogenously accumulated (resulting from the *aln* mutation) and exogenously applied allantoin caused an increase in leaf petiole ER bodies even in the absence of stress (Figure II-5). Thus, these results provided a link between the dynamic behavior of ER bodies and BGLU18 activation, supporting an idea that ER dynamics modulate BGLU18 activity, hence ABA production from ABA-GE.

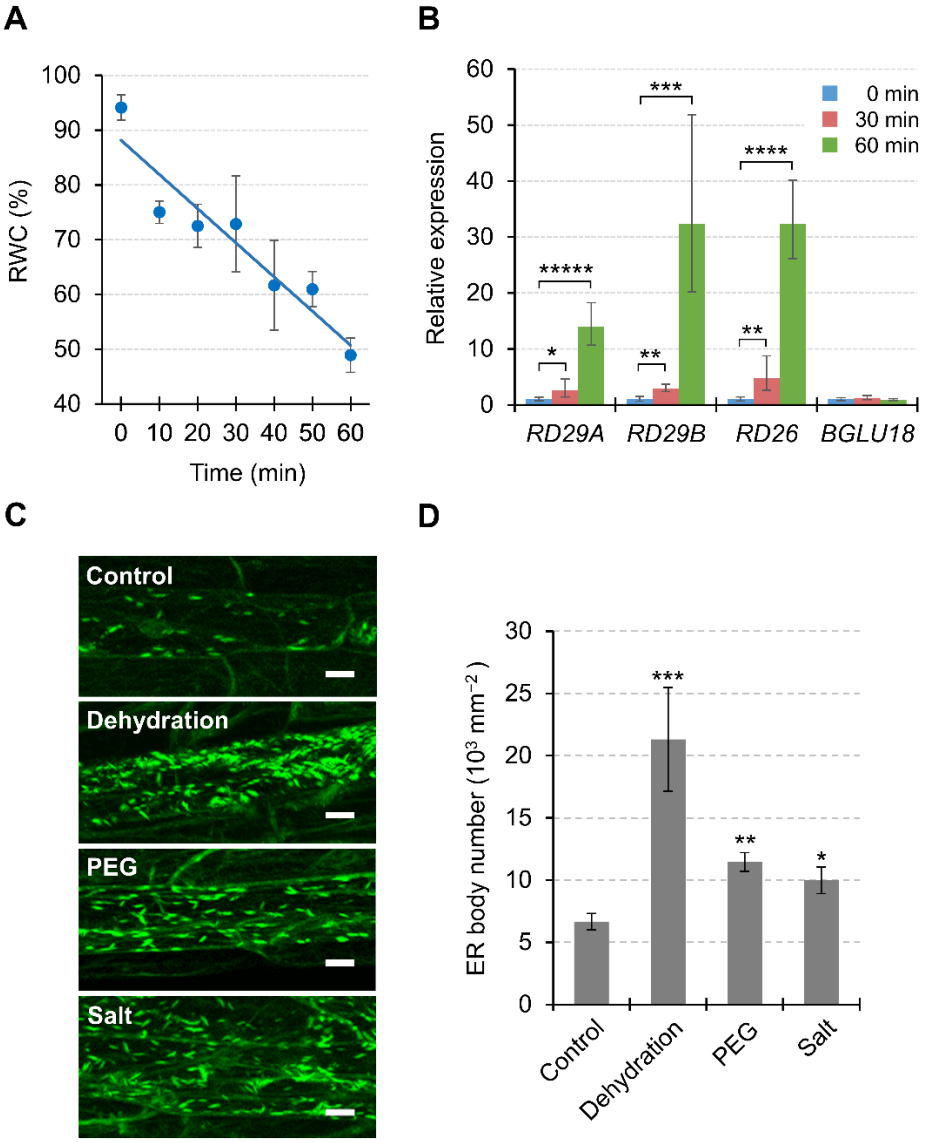

Figure II-1. Responses of ER bodies to abiotic stress in epidermal cells of Arabidopsis leaf petioles. (A) Effects of drought-induced dehydration stress on leaf relative water content (RWC). Aseptically grown plants were exposed to dry air for up to 60 min by removing the lids from Petri dishes, and leaves were detached for RWC measurements (n = 3, where each sample consisted of at least ten plants). The straight line corresponds to a linear model fitted to the measured data (y = –0.6235x + 88.148, r^2 = 0.8959, P < 0.005). (B) Effects of dehydration stress on stress-responsive gene expression. Total RNA was extracted at from the aerial parts of dehydration-stressed plants at the indicated time points. Transcript levels of target genes were measured by RT-qPCR, normalized to those of *SAND* as a reference gene, and represented as relative values to the level at the start of stress (0 min), which was given a value of 1. See Figure II-2 for the results using other reference genes. PCR primer sequences are provided in Table II-1. Data are means ± SD (n = 3), and asterisks denote significant differences between 0-min value and 30- or 60-min value in individual genes (*P < 0.05; **P < 0.005; ***P < 0.0005; ****P < 0.000005; *****P < 0.000001 by Student's t-test). (C) Representative fluorescent images of epidermal cells of *GFP-h* plants subjected to dehydration, PEG-mediated osmotic stress, or high salinity (Salt). Dehydration stress

(**Figure II-1** legend continued)
was applied as described for 60 min, while osmotic and salt stress was applied by transferring plants onto solid medium containing PEG (equivalent to −0.5 MPa) or 150 mM NaCl, respectively, and incubating for 12 hours. Scale bars = 20 μm. (D) Number of ER bodies in leaf petiole epidermal cells of *GFP-h* plants exposed to various stresses. Data are means ± SD ($n = 4$; *$P < 0.05$; **$P < 0.001$; ***$P < 0.00001$ by Student's *t*-test compared to the control.

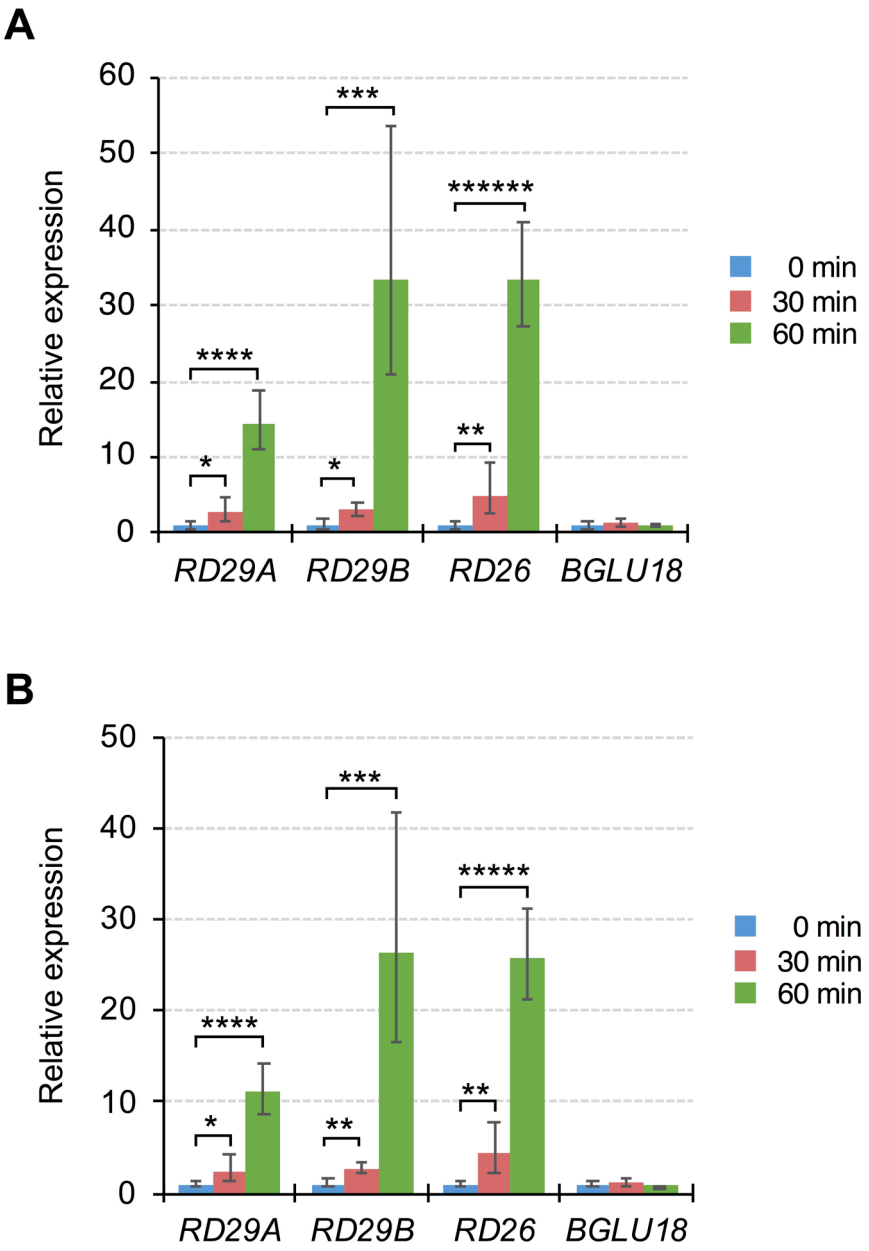

Figure II-2. Changes in relative transcript levels of stress-responsive genes during the progression of drought-induced dehydration. Aseptically grown 14-day-old plants were exposed to dehydration by removing the lid from the petri dishes for up to 60 min as described in the Materials and Methods section. Total RNA was extracted at indicated time points from aerial parts of drought-stressed plants. Transcript levels of target genes (*RD29A*, *RD29B*, *RD26*, and *BGLU18*) were determined by RT-qPCR, normalized to those of *PPR* (A) and *UBC9* (B) as reference genes, and represented as relative values to the level at the start of stress (0 min) which is given a value of 1. See Figure II-1B for the results of using *SAND* as reference. PCR primer sequences are provided in Table II-1. Data are means ± SD ($n = 3$) and asterisks denote significant differences between 0-min value and 30- or 60-min value in individual genes (*$P < 0.05$; **$P < 0.01$; ***$P < 0.005$; ****$P < 0.00005$; *****$P < 0.000001$; ******$P < 0.0000005$ by unpaired Student's *t*-test).

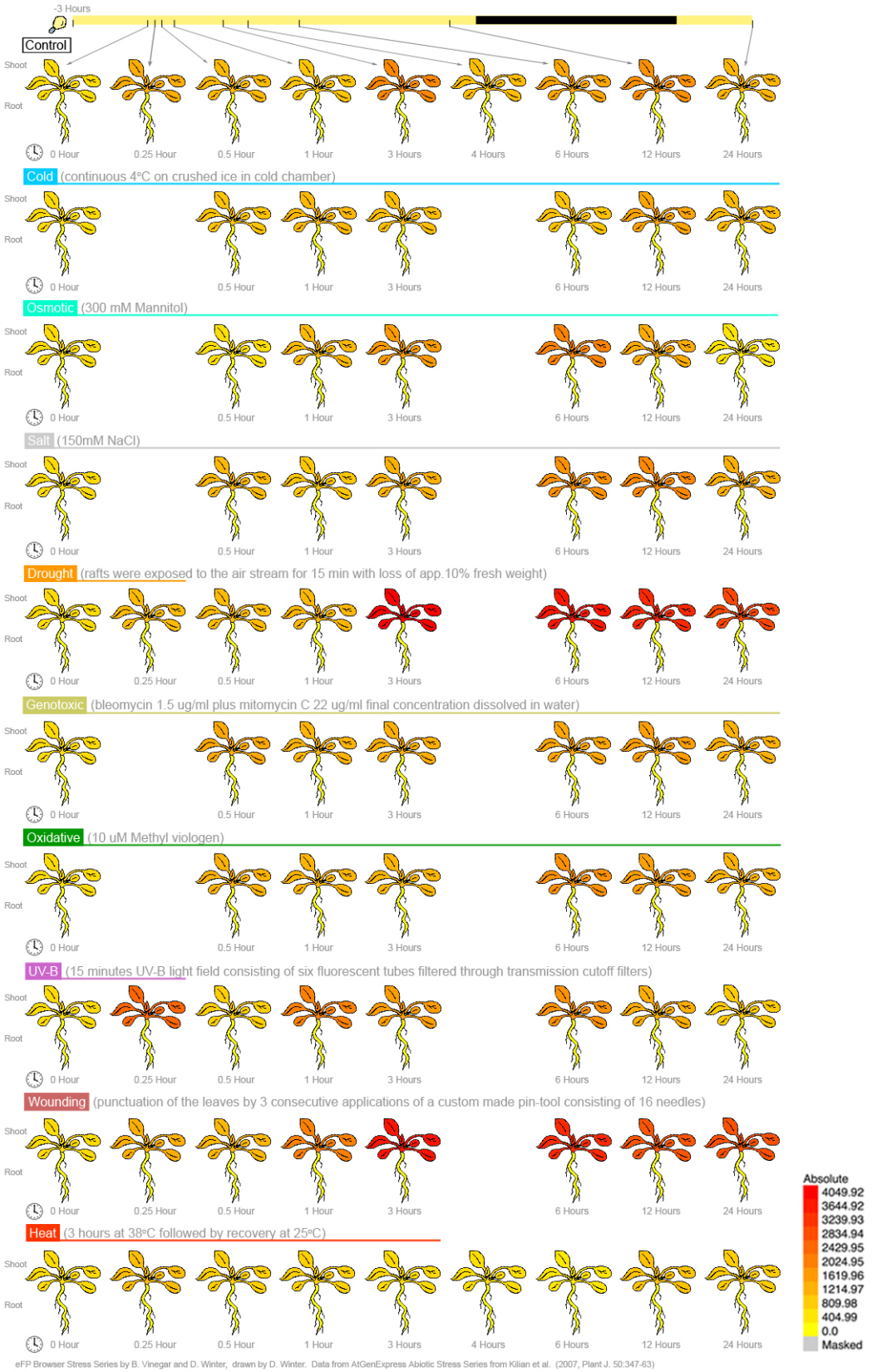

Figure II-3. Expression profile of the *BG1*/*BGLU18* gene (At1g52400) in Arabidopsis plants under various abiotic stress conditions. Obtained from the Arabidopsis eFP browser web server (http://bar.utoronto.ca/efp/cgi-bin/efpWeb.cgi) and reprinted from Winter *et al.* (2007).

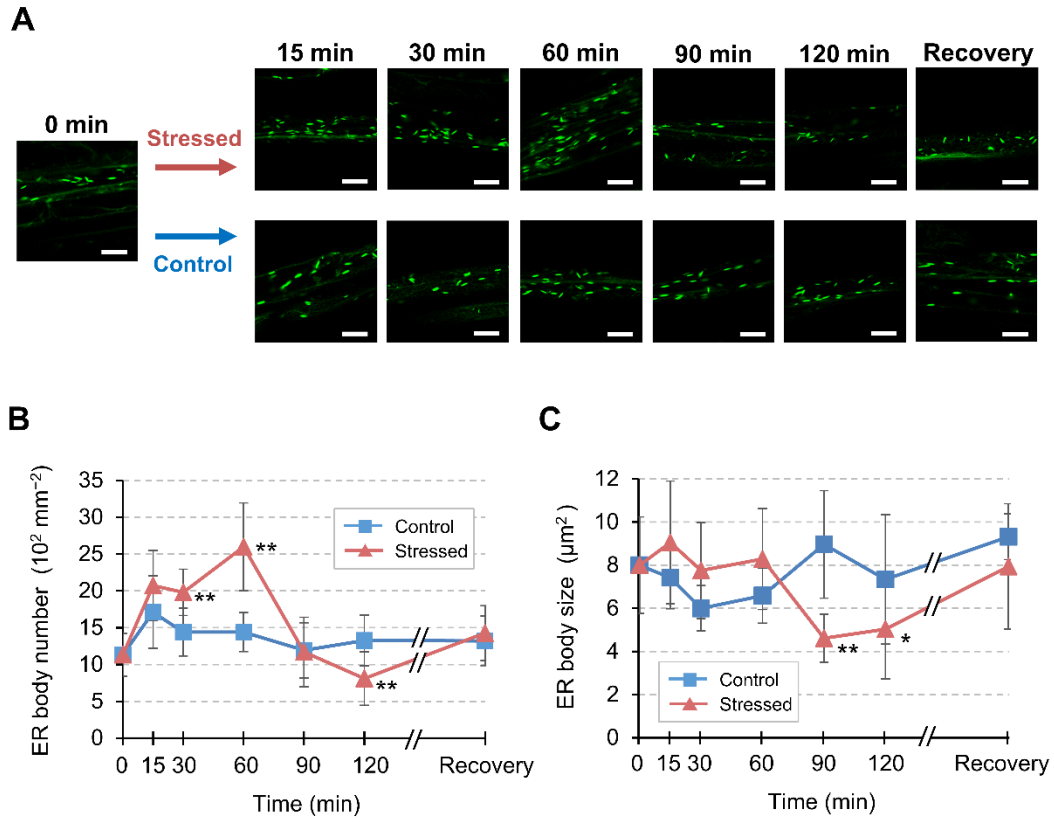

Figure II-4. Dynamic changes in leaf petiole ER bodies in response to drought-induced dehydration stress. (A) Representative time-course fluorescence images of leaf petiole epidermal cells of a *GFP-h* plant exposed to dehydration stress. Aseptically grown plants were subjected to dry air for the indicated time period up to 120 min. For recovery, stressed plants were restored to normal conditions and grown for an additional 18 hours. Scale bars = 20 μm. (B and C) Time-course of changes in the number (B) and average size (C) of ER bodies. Two-dimensional sizes of individual ER bodies, as indicated by green spot areas, were determined as described in the Materials and Methods. Data are means ± SD ($n = 4$ in B; $n = 5$ in C; $^{*}P < 0.05$; $^{**}P < 0.01$ by Student's *t*-test compared to the control at the same time point).

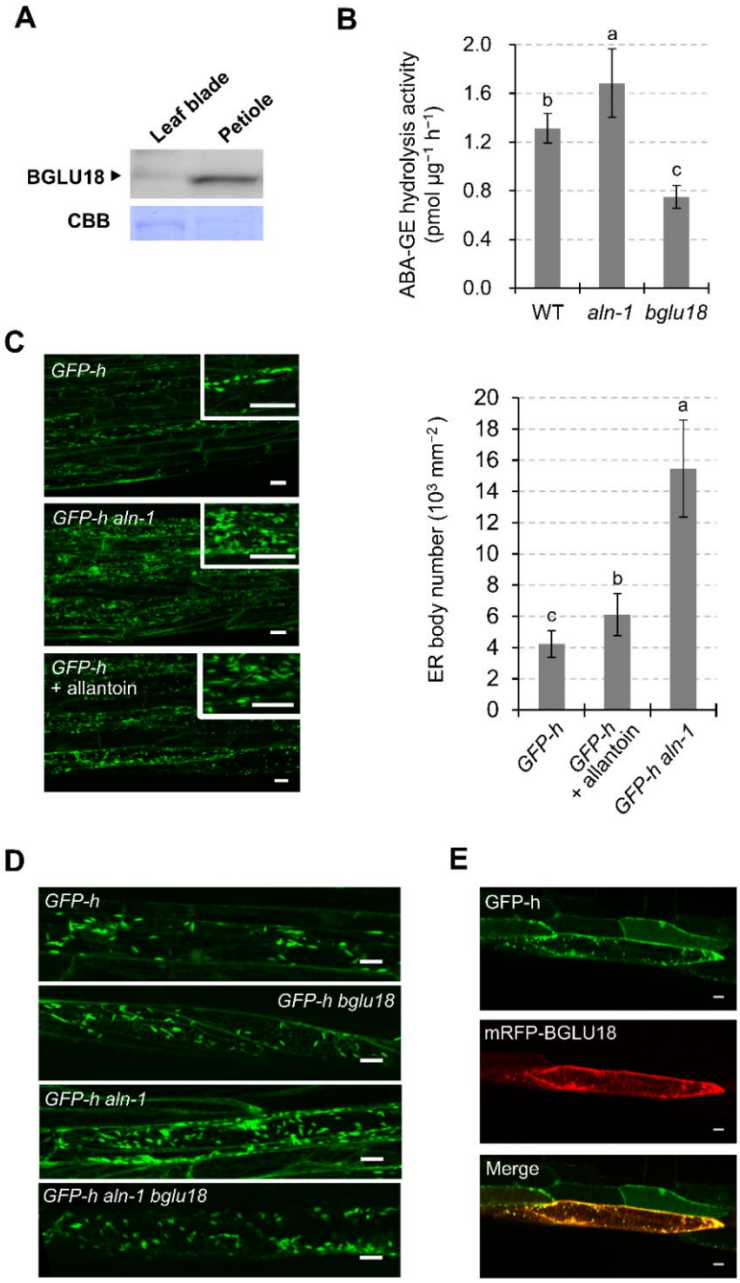

Figure II-5. Effects of *aln* mutation and exogenous allantoin on the ABA-GE activity of BGLU18 and ER bodies in leaf petioles. (A) Distribution of BGLU18 in *aln-1* leaf tissue. Immunoblotting was carried out as described in Figure I-4A. (B) ABA-GE hydrolysis activity in WT, *aln-1*, and *bglu18* plants. (C) Representative fluorescence images of leaf petiole epidermal cells in *GFP-h* (upper), *GFP-h aln-1* (middle), and *GFP-h* plants grown in the presence of 100 μM allantoin (lower). The histogram on the right shows the quantity of ER bodies in leaf petiole epidermal cells. (D) Representative fluorescence images of leaf petiole epidermal cells in *GFP-h* (uppermost), *GFP-h bglu18* (upper middle), *GFP-h aln-1* (lower middle), and *GFP-h aln-1 bglu18* plants (lowermost). (E) Representative fluorescence images of leaf petiole epidermal cells transiently expressing *mRFP-BGLU18* in *GFP-h aln-1* plants. Data are means ± SD (n = 3 in B; n = 5 in C). Different letters indicate a significant difference ($P < 0.05$ by one-way ANOVA). Scale bars = 20 μm.

Table II-1. Primers used in gene expression analysis by RT-qPCR.

AGI[a]	Gene symbol[b]	Direction	Sequence (Designation)	Use
At1g52400	*BG1*/*BGLU18*	Forward	5′-TGAGTGGCAAGATGGGTACA-3’	RT-qPCR
		Reverse	5′-TCAGCTTGGAGGTTGGAAAC-3’	RT-qPCR
At5g52310	*RD29A*	Forward	5′-AGGAACCACCACTCAACACA-3′	RT-qPCR
		Reverse	5′-ATCTTGCTCATGCTCATTGC-3′	RT-qPCR
At5g52300	*RD29B*	Forward	5′-ACGAGCAAGACCCAGAAGTT-3′	RT-qPCR
		Reverse	5′-AGGAACAATCTCCTCCGATG-3′	RT-qPCR
At4g27410	*RD26*	Forward	5′-AGTTCGATCCTTGGGATTTG-3′	RT-qPCR
		Reverse	5′-ACCCGTTGCTTTCCAATAAC-3′	RT-qPCR
At1g62930	*PPR*	Forward	5′-GAGTTGCGGGTTTGTTGGAG-3′	RT-qPCR (as reference)
		Reverse	5′-CAAGACAGCATTTCCAGATAGCAT-3′	RT-qPCR (as reference)
At2g28390	*SAND*	Forward	5′-AACTCTATGCAGCATTTGATCCACT-3′	RT-qPCR (as reference)
		Reverse	5′-TGATTGCATATCTTTATCGCCATC-3′	RT-qPCR (as reference)
At4g27960	*UBC9*	Forward	5′-TCACAATTTCCAAGGTGCTGC-3′	RT-qPCR (as reference)
		Reverse	5′-TCATCTGGGTTTGGATCCGT-3′	RT-qPCR (as reference)

[a] *Arabidopsis thaliana* gene identifier (AGI) code assigned according to the guidelines for nomenclature used for Arabidopsis genes (https://www.arabidopsis.org/portals/nomenclature/guidelines.jsp).

[b] Gene symbol, as provided by The Arabidopsis Information Resource (TAIR; release 10; https://www.arabidopsis.org/).

Table II-2. Mass spectrometry settings for the LC-ESI-MS/MS analysis of ABA in negative mode.

Analyte	Retention time on LC (min)	Molecular ion	Precursor ion (*m*/*z*)	Product ion (*m*/*z*)	Isolation width (*m*/*z*)	Ionization voltage (V)	Collision energy (eV)
ABA	5.5	$[M-H]^-$	263.12	153.1	2	10	30
d_6-ABA	5.5	$[M-H]^-$	269.13	159.1	2	10	30

CHAPTER III

The causal relationship between endoplasmic reticulum dynamics and stress-induced rapid ABA production mediated by BGLU18

Introduction

Two distinct pathways leading to stress-induced ABA production differs in their regulation. The *de novo* biosynthesis is primarily activated by transcriptional induction of genes encoding a set of plastidic and cytosolic enzymes including the rate-limiting NCED (Iuchi *et al*., 2000; Thompson *et al*., 2000; Xiong *et al*., 2002). On the other hand, a single-step deconjugation reaction catalyzed by BGLU18 and BGLU33 requires post-translational activation (Lee *et al*., 2006; Xu *et al*., 2012).

The activities of both BGLU18 and BGLU33 increase in response to dehydration. However, the mechanistic aspects behind the activation of these enzymes appear to differ. BGLU18 normally occurs as monomers that undergo multimerization, and thereby activation, in response to drought stress (Lee *et al*., 2006; Watanabe *et al*., 2014b), whereas BGLU33 normally exists as active, stable multimers whose levels increase upon exposure to stress (Xu *et al*., 2012). The difference in molecular regulation of the two

enzymes suggests the existence of organelle-specific activation mechanisms (i.e., ER versus vacuole) although such mechanisms have not been presented or demonstrated thus far.

In CHAPTER II, I showed that ER bodies responded to abiotic stresses by changing their number and shape. Moreover, such changes in ER bodies correlated with the activated status of BGLU18, supporting the idea of organelle-specific activation mechanisms. However, it is totally unknown as to the causal relationship between BGLU18 activation and the dynamic behavior of ER bodies upon exposure to stress. In addition, to the best of my knowledge, no studies have shown the subcellular localization of BGLU18 under stress conditions although under normal conditions, the enzyme is mainly stayed in ER bodies as I showed in the previous chapter. To address these issues, in this chapter, I examined whether the subcellular localization and activation status of BGLU18 were affected by changes in the ER-body status that are induced by drought-induced dehydration or *nai2-2* mutation which prevents ER-body formation. Finally, I investigated the contribution of BGLU18 in stress-induced rapid ABA production by monitoring and comparing the kinetics of dehydration-induced ABA accumulation in leaves between WT and ABA-metabolic mutants, such as *aba2-1* and *bglu18*, impaired in the *de novo* synthesis and ABA-GE hydrolysis, respectively.

Material and methods

Plant materials and growth conditions

The plant materials and growth conditions are described as in CHAPTER I. The seeds of the following SALK T-DNA insertion lines were obtained from the Arabidopsis Biological Resource Center (Ohio State University): *aba deficient2-1* (*aba2-1*; CS156; Léon-Kloosterziel *et al*., 1996) for *ABA2* (At1g52340), and *nai2-2* (SALK_005896; Yamada *et al.*, 2008) for *NAI2* (At3g19590). The *bglu18 nai2-2* double mutant was obtained by crossing the respective single mutants. Two transgenic lines, *GFP-h* and *GFP-h nai2-2*, which express green fluorescent protein (GFP) with an ER-retention signal, HDEL (GFP-h), in the WT and *nai2-2* backgrounds, respectively, were described by Hayashi *et al*. (2001) and Yamada *et al*. (2008). These *GFP-h* lines were crossed with some of the above-mentioned mutants to allow ER/ER bodies to be visualized in each genetic background. To identify homozygous T-DNA insertion lines, I performed PCR-based genotyping of each mutant using gene-specific primers as shown in TABLE III.

Protein extraction, SDS-PAGE and western blotting

The extraction of proteins, SDS-PAGE and Western blotting were performed as described in CHAPTER I.

Transient expression assay

The transient assay by particle bombardment were carried out as described in CHAPTER I.

Stress treatments

Drought-induced dehydration stress was applied to plants as described in CHAPTER II

ABA quantification and measurement of ABA-GE hydrolysis activity

The procedures for the experiments are described in CHAPTER II.

Statistical analysis

Results are presented as means with SD from at least three independent experiments, unless otherwise noted. Statistical analysis was performed as described in CHAPTER II.

Results

BGLU18 remains in the ER and enhances ABA-GE hydrolysis activity to increase ABA levels under dehydration stress

ER bodies are subcellular compartments that function in the temporary storage of certain BGLUs, such as BGLU23, which are released from the ER bodies upon stress to react with substrates stored separately in other compartments, such as vacuoles (Yamada *et al*., 2011; Nakano *et al.*, 2014). Whether the BGLU18 substrate, ABA-GE, is stored in the ER is unclear, although it forms in the cytosol and is transported into the vacuole for intracellular storage (Harris and Dugger, 1986; Burla *et al*., 2013; Dong *et al*., 2014).

Therefore, I investigated whether abiotic stress affects the subcellular localization of BGLU18. When I exposed *GFP-h* plants transiently expressing *mRFP-BGLU18* to a 30-min dehydration stress (Figure II-4), the ER status of the stressed cells was significantly altered compared to that of control cells (Figure III-1A, left of the left panel). Under stress conditions, mRFP signals, which overlapped fully with GFP signals under control conditions, had slightly diffused from major GFP spots (ER bodies) and became a bit more evenly distributed within the cell (Figure III-1A, middle and right of the left panel). This observation was supported by quantitative analysis of relative

fluorescence intensities across the cell (Figure III-1A, right panel). I also examined the distribution of endogenous BGLU18 in subcellular fractions obtained from dehydration-stressed plants by immunodetection. Dehydration treatment increased the level of BGLU18 in the microsomal P100 fraction, albeit to a small extent, suggesting that stress affects the relative distribution of BGLU18 between ER bodies and microsomes (consisting of ER membranes and lumen proteins) (FigureIII-1B). However, the protein was barely detected in the S100 fraction, indicating that BGLU18 primarily remains in the ER and ER bodies under dehydration stress.

I investigated whether these changes in distribution occurred in conjunction with changes in the ABA-GE hydrolysis activity of BGLU18 and with ABA levels in the leaf petiole. BGLU18 activity significantly increased in WT plants exposed to dehydration compared to non-stressed plants, whereas BGLU18 activity in *bglu18* was similar under both conditions (Figure III- 1C). ABA-GE hydrolysis activity in WT was estimated to increase three-fold when background *bglu18* activity was subtracted from each condition. Along with increasing enzyme activity, ABA levels significantly increased (two-fold) in leaf petioles from stressed plants. Overall, these results uncover a link between stress-induced ER dynamics, BGLU18 activation, and ABA levels.

Loss of constitutive ER bodies enhances BGLU18 activity under normal

and dehydrated conditions, but ABA levels increase only under dehydrated conditions

To further investigate the causal relationship between the changes in BGLU18 distribution in the ER system and increased BGLU18 activity and ABA levels under dehydration stress, I examined the *nai2-2* mutant, which is deficient in constitutive ER bodies. Since this mutation has little or no effect on BGLU18 protein levels (Figure III-2), I predicted that the loss of constitutive ER bodies, which accumulate BGLU18 (Figure I-4), would result in the increased distribution of this enzyme to microsomes under normal conditions. Consistent with the results described above (Figure III-1B), WT plants contained more BGLU18 in the ER-body-rich P1 and P8 fractions than in the microsomal P100 fraction (Figure III-3). By contrast, in *nai2-2*, BGLU18 was distributed nearly evenly between the three fractions. These results indicate that the relatively high levels of BGLU18 in the microsomes of *nai2-2* are due to its inability to form constitutive ER bodies.

I measured ABA-GE hydrolysis activity and leaf petiole ABA levels in *nai2-2*, along with the *bglu18 nai2-2* double mutant as a background control (Figures III-3 and III-4), and compared these results with those for the WT and *bglu18* single mutant (Figure III-3B). The *nai2-2* plants showed the highest and the *bglu18* plants the lowest ABA-GE hydrolysis activity under

both normal and stress conditions (Figure III-3B). Introducing the *bglu18* mutation into the *nai2-2* background resulted in lower enzyme activity in the *bglu18 nai2-2* double mutant compared to *nai2-2* single mutant plants, suggesting that the *nai2-2* mutation caused increased activity of BGLU18 and possibly other enzymes capable of degrading ABA-GE. Along with enzyme activity, dehydration stimulated ABA accumulation by five-fold in *nai2-2* (Figure III-3B, lower) to a level significantly higher than that in WT (two-fold increase). Under normal conditions, however, this increased enzyme activity did not lead to increased ABA levels in *nai2-2*. Neither the *bglu18* single nor *bglu18 nai2-2* double mutant responded to dehydration-stress treatment by increasing ABA levels, suggesting that *de novo* synthesis contributed little to increased ABA levels under my experimental conditions, as examined further below. These results indicate that dehydration-responsive ABA production occurs in leaf petioles, a process mediated by BGLU18 and augmented by the loss of constitutive ER bodies, but this occurs only under stress conditions.

Loss of BGLU18 causes a delay in dehydration-induced ABA accumulation

To examine the temporal and spatial contribution of BGLU18 to the early stage of stress-induced ABA accumulation, I monitored changes in ABA levels in the leaf tissue of WT plants and two ABA-metabolism mutants, *bglu18*, and *aba2-1*, during a 120-min dehydration treatment

(Figure III-5). ABA levels in WT petioles significantly increased (more than two-fold) within 30 min of the onset of stress treatment and continued to increase (5.8-fold) by 120 min of treatment, whereas they remained steady under control conditions (Figure III-5A, upper panel). In dehydration-stressed *bglu18* petioles, the ABA levels did not increase significantly until 60 min ($P > 0.3$ by one-way ANOVA) and then increased 4.6-fold at 120 min, revealing the delayed increase in ABA accumulation in the absence of BGLU18. ABA levels in *aba2-1*, which is impaired in *de novo* ABA biosynthesis, were only 8–11% and 12–20% those of the WT and *bglu18*, respectively, under control conditions. However, ABA levels increased slightly but significantly (1.2-fold) within the first 30 min of dehydration treatment (Figure III-5A, lower panel), suggesting that ABA-GE hydrolysis contributes to the early response to dehydration stress, which is likely mediated by BGLU18. ABA levels in leaf blades of the three genotypes exhibited a similar pattern to those in the petiole under both control and stress conditions, with slightly higher levels in leaf blades vs. petioles (Figure III-5B). Taken together, these results indicate that BGLU18 is involved in an early stage of ABA accumulation not only in the petioles but also in the blades of dehydration-stressed leaves.

Discussion

In this chapter, I further explored the relevance of ER dynamics to BGLU18 activation, as ER bodies were previously considered to be physiologically inert (Herman and Schmidt, 2004; Yamada *et al.*, 2011; Nakano *et al*., 2014). In contrast to NAI2, an ER-body-specific protein (Yamada *et al*., 2008), BGLU18 was not exclusively localized to ER bodies; a certain amount was detected in the microsomal (ER) fractions under normal conditions (Figure I-4B). Intriguingly, drought-induced dehydration stress not only triggered changes in ER-body status but also led to a relative increase in BGLU18 levels in microsomes, resulting in enhanced ABA-GE hydrolysis activity and increased ABA concentrations (Figure III-1). By contrast, under the experimental conditions used here, neither enzyme activity nor ABA levels were altered in the *bglu18* mutant exposed to the same stress treatment. These results suggest that stress-induced ER-body dynamics somehow enhance BGLU18-mediated ABA production by affecting the relative distribution of the enzyme between ER and ER bodies. The mechanisms causing such sub-ER distributional changes in BGLU18 are currently unknown. Notably, upon exposure to dehydration, the size of ER bodies decreased following a transient increase in their numbers (Figure II-4).

Perhaps ER bodies undergo partial degradation or disorganization to liberate BGLU18 into the ER, where catalysis might occur. I tested this

possibility using an ER body-deficient *nai2-2* mutant. I reasoned that BGLU18 would reside in the ER if the formation of constitutive ER bodies were prevented by the *nai2-2* mutation, as the mutation did not affect BGLU18 protein levels. Compared to WT, BGLU18 was relatively enriched in microsomes in the *nai2-2* mutant, where ABA-GE hydrolysis activity was significantly higher under both normal and stress conditions (Figure III-3). These results suggest that the disorganization of the ER body represents a key process for BGLU18 activation. Despite the increased enzyme activity, however, this mutant over-accumulated ABA only when exposed to stress (to a level more than three-fold higher than that of equally stressed WT; Figure III-3B). Similarly, Lee *et al*. (2006) demonstrated that constitutive BG1/BGLU18 overexpression in Arabidopsis profoundly increased foliar ABA levels under dehydration stress but not control conditions. The results here support the idea that ABA-GE is not normally stored in the ER but is transported there from the apoplast and/or vacuoles via a yet unknown stress-stimulated mechanism (Dietz *et al*., 2000; Lee *et al*., 2006). Alternatively, as ER bodies function in ER-to-vacuole trafficking pathways (Hayashi *et al*., 2001; Herman and Schmidt, 2004), it is conceivable that upon stress exposure, BGLU18 is transported to the vacuole, where it hydrolyzes ABA-GE. However, this is unlikely given my findings on mRFP-BGLU18 localization under dehydration stress (Figure III-1A).

An obvious advantage of ABA production from ABA-GE lies in its

status as a single-step reaction, which occurs much more rapidly than the multi-step process of ABA biosynthesis. Thus, BGLU18 is thought to enable the rapid production of ABA in order to increase cellular levels locally rather than overall (Lee *et al*., 2006). My finding that BGLU18 activation occurs shortly (30 min) after the onset of dehydration stress (Figures III-1 & 3) is consistent with this hypothetical role of BGLU18, and hence ABA-GE hydrolysis, in stress responses. This idea was further supported by my time-course comparison of dehydration-induced ABA accumulation in leaves among genotypes, as the *bglu18* mutant did not exhibit the early ABA accumulation that was observed in WT (Figure III-5). Conversely, the *aba2-1* mutant showed slightly but significantly earlier ABA production in response to dehydration, even though *de novo* ABA synthesis is largely impaired in this mutant. This small but early increase likely results from the deconjugation of ABA-GE. These results strongly suggest that the rapid activation of BGLU18 is responsible for the early ABA accumulation that precedes *de novo* biosynthesis, which might occur via a mechanism involving ER dynamics at the organellar level (this study) and post-translational regulation at the molecular level (Lee *et al*., 2006; Watanabe *et al*., 2014b); however, the transcriptional activation of *BGLU18* is unlikely based on RT-qPCR (Figure II-2). The time-course ABA analysis also revealed that BGLU18-mediated ABA-GE hydrolysis plays substantial roles in both the petioles and blades of stressed leaves.

The physiological significance of ABA production in the epidermal cells of leaf petioles remains to be addressed. My results suggest that ABA-GE hydrolysis plays a part in an early stress response to generate ABA, which might contribute to activation of the ABA biosynthetic pathway through positive feedback regulation (Xiong *et al*., 2002). Such feedback regulation would involve the translocation of ABA from BGLU18-containing epidermal cells to vascular parenchyma cells, where the genes for ABA-biosynthetic enzymes are primarily expressed (Koiwa *et al*., 2004; Endo *et al*., 2008; Kuromori *et al.*, 2014). The thin, stalk-like structure of the leaf petiole may be favorable for the translocation of ABA since epidermal tissues surround the vascular tissues in closer proximity in petioles compared to leaf blades.

BG1/BGLU18 was originally identified as an ER enzyme involved in ABA homeostasis and metabolism (Lee *et al*., 2006). However, this enzyme was recently proposed to act as a myrosinase to produce defense compounds from glucosinolate substrates in response to herbivory (Nakazaki *et al*., 2019). Given that ER bodies in leaves respond to both abiotic and biotic stress (Matsushima *et al*., 2002; this work), it is likely that BGLU18 plays a dual role, depending on which environmental stress the plant encounters. Since BGLU18 is physically separated from its substrates (*i.e.*, ABA-GE and indole glucosinolates) under normal conditions, the two distinct activities are likely regulated by the physiological process by which each substrate becomes available

under stress conditions: as noted above, dehydration-induced ABA production might involve stress-activated transport of ABA-GE into the ER from the apoplast or vacuoles (Lee *et al*., 2006; this work), whereas wounding-induced production of toxic compounds is achieved via the direct access of the enzyme to vacuole-resident glucosinolates upon cell collapse (Yamada *et al.*, 2011; Nakano *et al*., 2017). If this scenario is accurate, BGLU18 in leaf petioles might also be involved in defense against biotic stress, as it is in leaf blades.

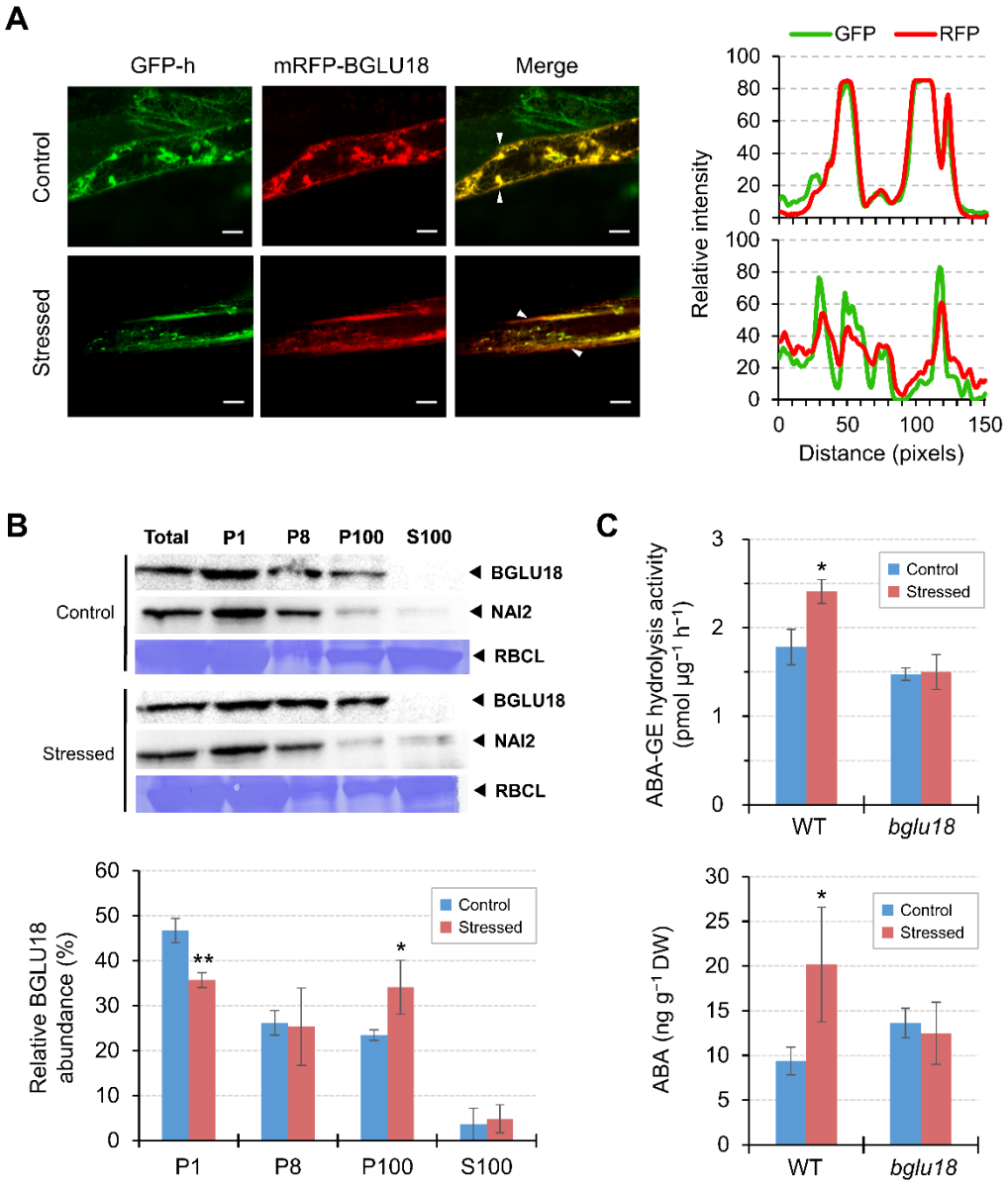

Figure III-1. Effects of drought-induced dehydration on the subcellular distribution and ABA-GE hydrolysis activity of BGLU18 and ABA levels in leaf petioles. (A) Left, representative fluorescence images of leaf petiole epidermal cells transiently expressing *mRFP-BGLU18* in *GFP-h* plants under control or stress conditions (as in Figure II-4 for 30 min). Scale bars = 20 μm. Right, line profile graphs showing relative pixel intensities for GFP (green) and mRFP (red) fluorescence (upper, control; lower, stressed), which were line-scanned and quantified between the two white arrowheads in the merged panels on the left using ImageJ. (B) Subcellular distribution of BGLU18. Biochemical fractionation followed by immunoblotting was performed starting with control plants and plants exposed to dehydration for 30 min. Bar graphs below show the relative distribution of BGLU18 in the four fractions. (C) ABA-GE hydrolysis activity (upper) and ABA levels (lower) in WT and *bglu18* plants under control conditions or exposed to dehydration for 30 min. Leaf petioles were collected from control and dehydration-stressed plants of each genotype and assayed for ABA by LC-ESI-MS/MS on a dry weight (DW) basis. Data are means ± SD ($n = 3$ in both B and C). Significant differences between treatments are indicated by asterisks (*$P < 0.05$; **$P < 0.005$ by Student's *t*-test).

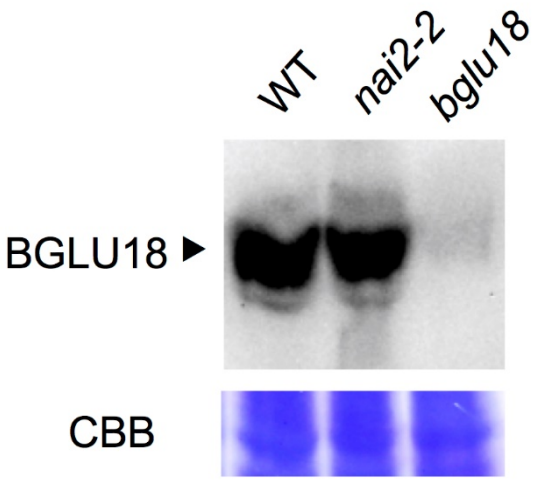

Figure III-2. BGLU18 protein levels in WT, *nai2-2*, and *bglu18* mutants. Immunoblotting was performed with anti-BGLU18 antibodies for proteins extracted from leaves of 14-day-old plants grown under normal conditions.

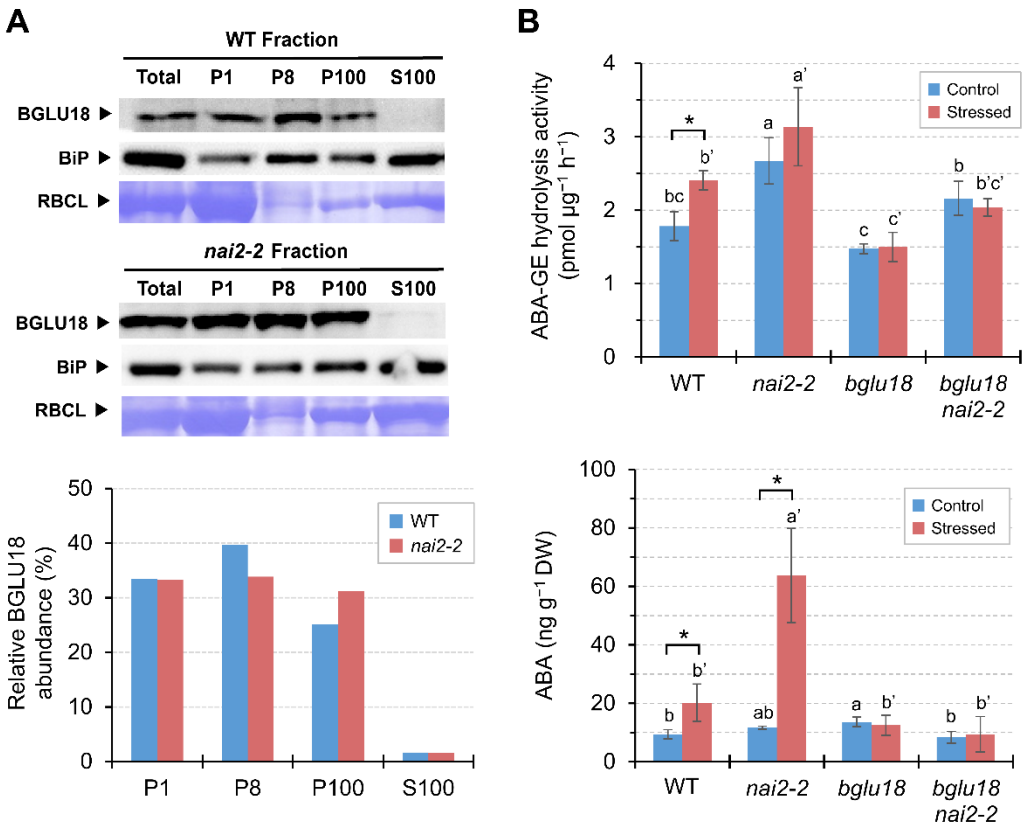

Figure III-3. Effects of *nai2* mutation on the subcellular distribution and ABA-GE activity of BGLU18 and on ABA levels in leaf petioles. (A) Subcellular distribution of BGLU18. Biochemical fractionation followed by immunoblotting analysis were performed as described in Figure I-4B. Bar graphs below show the relative distribution of BGLU18 in the four fractions. The experiments were repeated twice with similar results; results from one experiment are shown. (B) ABA-GE hydrolysis activity (upper) and ABA levels (lower) in *nai2-2* single and *nai2-2 bglu18* double mutant plants under control conditions or exposed to dehydration for 30 min. WT and *bglu18* data used for comparison are from Figure III-1C, as the experiments were done in parallel. Leaf petioles were collected from control and dehydration-stressed plants and assayed for ABA by LC-ESI-MS/MS on a dry weight (DW) basis. Data are means ± SD ($n = 3$). Significant differences between treatments are indicated by asterisks (*$P <$ 0.05 by Student's *t*-test) and those among genotypes by different letters ($P < 0.05$ by one-way ANOVA).

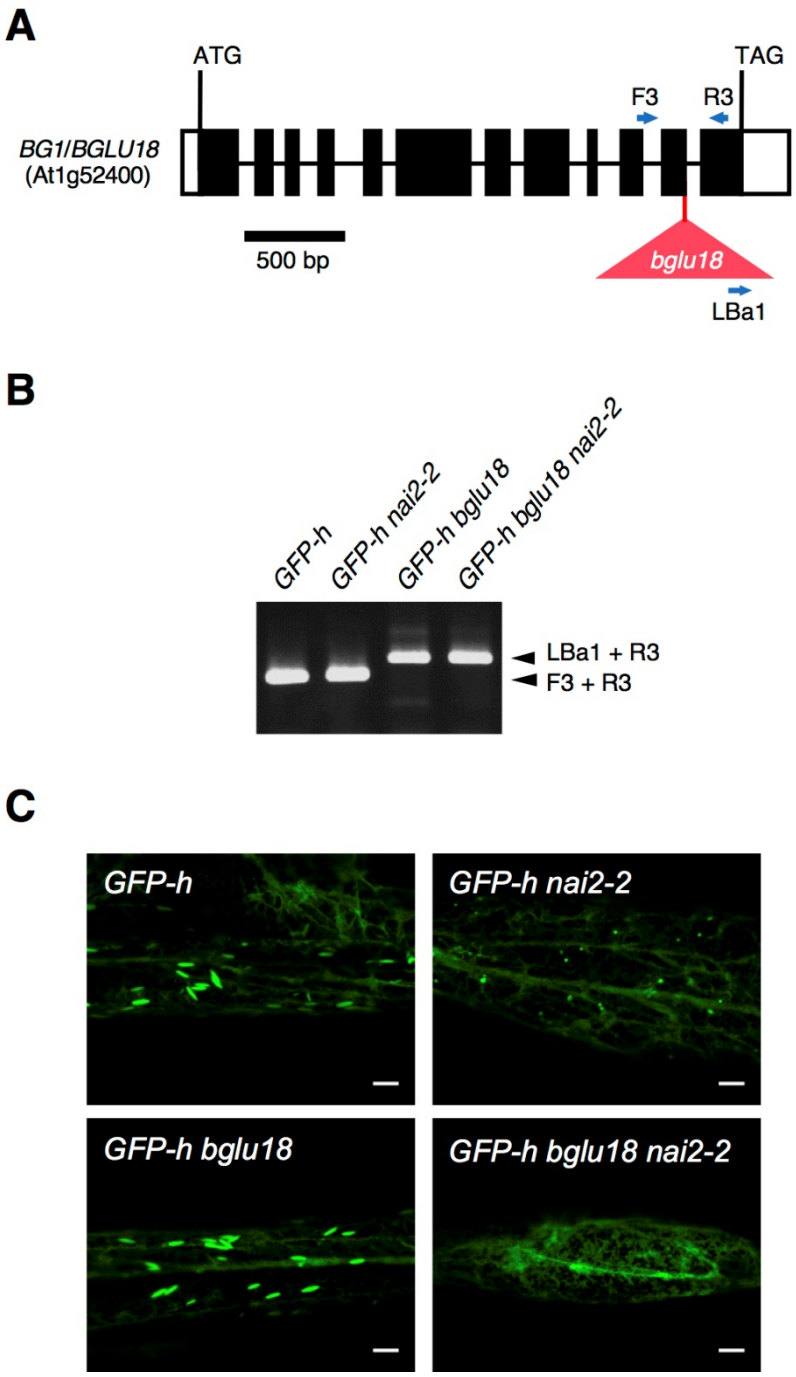

Figure III-4. Genotyping and phenotyping of a *bglu18 nai2-2* double mutant. The homozygous mutants of *bglu18* (SALK_075731C; Ogasawara *et al.*, 2009) and *nai2-2* (SALK_005896; Yamada *et al.*, 2008) were crossed to obtain the double mutant *bglu18 nai2-2*. All mutants express *GFP-h* to visualize ER/ER bodies. (A) Diagram of the T-DNA insertion in *BG1*/*BGLU18* (At1g52400) in the *bglu18* mutant. Arrows denote PCR primers. (B) PCR-based genotyping of the double mutant using primers specific to *BGLU18* (F3 and R3) and the left border sequence of T-DNA (LBa1). The sequences of primers are listed in Supplementary Table S1. (C) Representative GFP fluorescence images of leaf petiole epidermal cells. Scale bars = 10 μm.

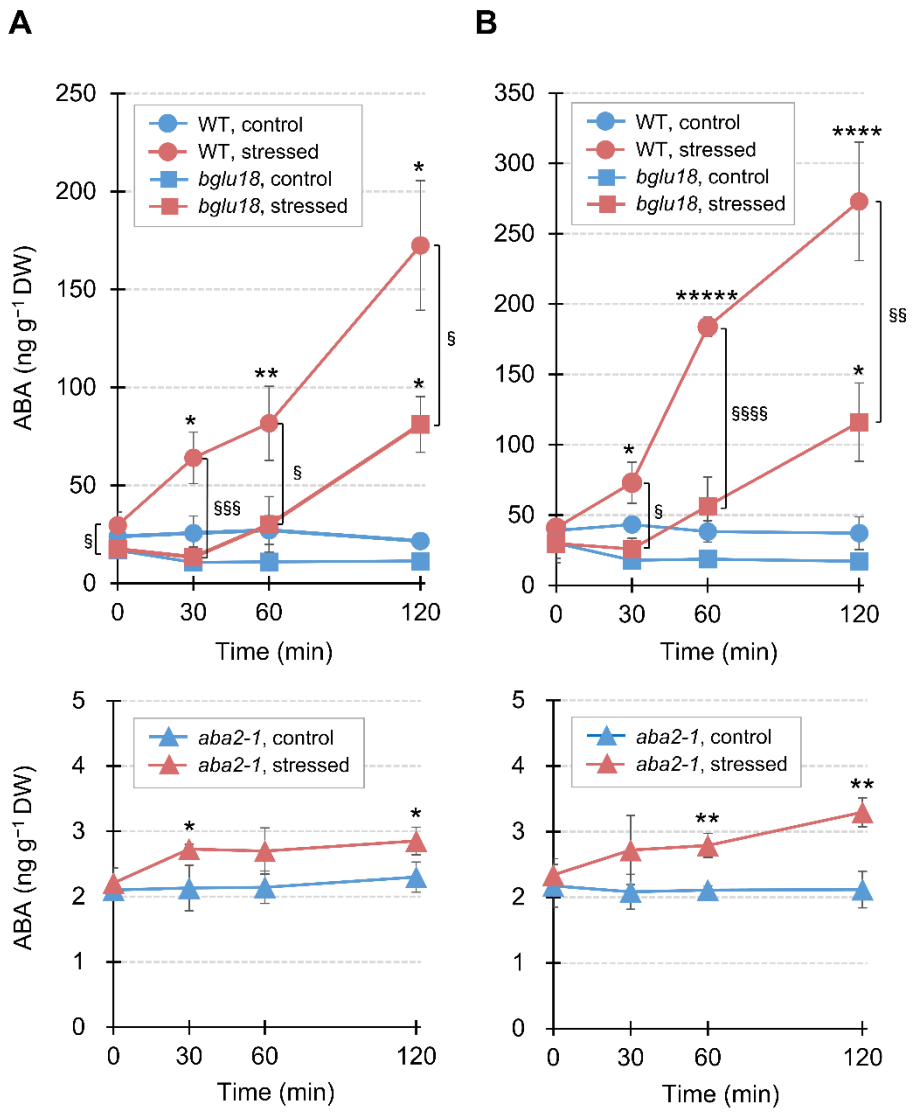

Figure III-5. Effects of *bglu18* and *aba2-1* mutations on time-course changes in dehydration-induced ABA accumulation in leaf petioles and blades. Aseptically grown plants were subjected to dry air for the indicated time periods up to 120 min, and leaf petioles (A) and blades (B) were separately collected for ABA measurements by LC-ESI-MS/MS on a dry weight (DW) basis. Data are means ± SD (n = 3). Significant differences between treatments are indicated by asterisks (*P < 0.05; **P < 0.01; ***P < 0.005; ****P < 0.001; *****P < 0.00005 by Student's t-test) and those between genotypes by section marks ($^{§}P$ < 0.05; $^{§§}P$ < 0.01; $^{§§§}P$ < 0.005; $^{§§§§}P$ < 0.001 by Student's t-test).

Table III. Primers used for genotyping *bglu18 nai2-2* double mutants.

AGI[a]	Gene symbol[b]	Direction	Sequence (Designation)	Use
At1g52400	*BG1*/*BGLU18*	Forward	5′-GGCGACCCAGAAGTTATCAT -3′ (F3)	PCR genotyping
		Reverse	5′-GAATACCATTTGCCCGAAAC-3′ (R3)	PCR genotyping
–	T-DNA	–	5′-TGGTTCACGTAGTGGGCCATCG-3′ (LBa1)	PCR genotyping

[a] *Arabidopsis thaliana* gene identifier (AGI) code assigned according to the guidelines for nomenclature used for Arabidopsis genes (https://www.arabidopsis.org/portals/nomenclature/guidelines.jsp).

[b] Gene symbol, as provided by The Arabidopsis Information Resource (TAIR; release 10; https://www.arabidopsis.org/), except for T-DNA of *Agrobacterium tumefaciens*.

GENERAL CONCLUSIONS

The regulation of ABA accumulation is of fundamental importance for plant responses to abiotic stresses such as drought. Although roots are the primary sites for sensing drought, there is evidence that the foliar production of ABA is independently required to elicit stress responses in leaves (Holbroock *et al*., 2002; Christmann *et al*., 2007). However, in contrast to the extensive research on the multistep process of *de novo* ABA biosynthesis, far fewer studies have investigated the single-step hydrolysis of ABA-GE, which allows for quick ABA production. To explore the cellular mechanism for the activation of foliar ABA production, I focused on BGLU18, a key enzyme for ABA-GE hydrolysis, in drought-stressed Arabidopsis leaves (Lee *et al*., 2006; Watanabe *et al*., 2014b).

In CHAPTER I, I found that BGLU18 was predominantly accumulated in the petiole of Arabidopsis leaves. By subcellular fractionation experiments and transient expression of the mRFP-tagged fusion protein, I showed that BGLU18 is mainly localized to ER bodies in the leaves, in contrast to the previous results reporting its localization in the ER (Lee *et al*., 2006). I also found the constitutive existence of ER bodies in true leaves although this stress-associated ER-derived structure had previously been reported only in the cotyledons and roots of mature plants when grown normally. These results suggested that the petiole is the main part of BGLU18-mediated ABA production in the leaves, and that ER bodies might participate in the modulation of BGLU18 activation

under stress.

In CHAPTER II, I revealed that the ER bodies responded significantly to abiotic stress such as drought-induced dehydration, osmotic stress and high salt conditions, by increasing their number in stressed leaf petiole cells. The detailed time-course analysis showed that the ER bodies responded to dehydration stress by increasing their number within 60 min and by reducing their size within 90 min. Interestingly, upon the removal of stress, the number and size of ER bodies returned to the original status, suggesting that such dynamic behavior of ER bodies is a physiological response to cope with abiotic stress conditions. Examining the effect on ER bodies of *aln* mutation and exogenous allantoin, both of which are known to activate BGLU18 under normal conditions (Watanabe *et al*., 2014b), revealed that the increased number of ER bodies correlates with the increase in BGLU18 activity. These results indicate that ER bodies might participate in the regulation process of BGLU18 activation under abiotic stress.

In CHAPTER III, I reported that under dehydration stress, the significant fraction of BGLU18 shifted from ER bodies to the ER. Notably, this distributional shift was accompanied by increasing BGLU18-mediated ABA-GE hydrolytic activity and ABA levels in leaf petioles, leading to an idea that the stress-induced distributional change within the ER network is a key process for activation of BGLU18 under stress. I tested this idea by using *nai2-2* mutants since they lack ER bodies and thus contain most of BGLU18 in the ER. As expected, *nai2-2*

mutants increased BGLU18 activity even under non-stress conditions; however, ABA levels increased only under stress, probably because ABA-GE is supplied to the ER only under these conditions through the yet-unknown mechanism that is stimulated by stress. The time-course analysis of ABA accumulation under stress revealed that ABA-GE hydrolysis precedes *de novo* biosynthesis in an early stress response to generate ABA, which might contribute to activation of the biosynthetic pathway through positive feedback regulation. This analysis also showed that BGLU18-mediated ABA-GE hydrolysis plays a substantial role not only in the petioles but also blades of stressed leaves.

Finally, the results presented in this thesis demonstrate the involvement of ER dynamics in stress-induced rapid ABA production mediated by BGLU18, which has intriguing implications for the regulation of cellular ABA metabolism and homeostasis during stress responses and adaptation in plants. This study also sheds light on the novel physiological functions of ER bodies, which still remain to be fully explored.

Acknowledgements

This study was carried out in Laboratory of Molecular Plant Biology, Department of Mathematical and Life Sciences, Graduate School of Science, Hiroshima University.

I would like to express my sincere appreciation to Professor Atsushi Sakamoto, Hiroshima University, for giving me the chance to perform this study, and for his patient guidance, discussion, invaluable suggestion and constant support. I am especially grateful for his understandings and concerns, which would be the best encouragement for foreign student that study in Japan.

I thank Professor Emeritus Mikio Nishimura (National Institute for Basic Biology) and Professor Ikuko Hara-Nishimura (Konan University) for providing the *GFP-h* transgenic lines and antibodies against BGLU18, NAI2, and BiP, and their colleagues for their valuable suggestions and discussion; and Prof. Tsuyoshi Nakagawa (Shimane University) for pUGW2. I thank Ms. Tomoko Amimoto, the Natural Science Center for Basic Research and Development (N-BARD), Hiroshima University, for the technical assistance of ABA measurements.

I wish to thank Associate Professor Hiroshi Shimada and Assistant Professor Misa Takahashi, Hiroshima University, Dr. Shunsuke Watanabe, RIKEN Center for Sustainable Resource Science, and Dr. Hiroshi Takagi, University of Minnesota for their

valuable advices, collaboration, and warm encouragements.

I am profoundly grateful to all past and current members of Laboratory of Molecular Plant Biology. Particularly, I thank Messrs. Shoma Tanaka, Daichi Kinoshita, and Yuhi Hashiguchi, for their collaboration and technical assistance.

I am indebted to China Scholarship Council, China, for awarding me the scholarship for Abroad Chinese Doctor Students (CSC No. 201508050080) during the course of the doctoral program.

Finally, I would like to greatly appreciate my family and friends for their support and encouragement throughout my study.

References

Almeida Trapp M, De Souza GD, Rodrigues-Filho E, Boland W, Mithöfer A. 2014. Validated method for phytohormone quantification in plants. Frontiers in Plant Science **5**, 417.

Barrs HD, Weatherley PE. 1962. A re-examination of the relative turgidity technique for estimating water deficit in leaves. Australian Journal of Biological Sciences **15**, 413–428.

Burla B, Pfrunder S, Nagy R, Francisco RM, Lee Y, Martinoia E. 2013. Vacuolar transport of abscisic acid glucosyl ester is mediated by ATP-binding cassette and proton-antiport mechanisms in Arabidopsis. Plant Physiology **163**, 1446–1458.

Cheng WH, Endo A, Zhou L, Penney J, Chen HC, Arroyo A, Leon P, Nambara E, Asami T, Seo M, Koshiba T, Sheen J. 2002. A unique short-chain dehydrogenase/reductase in Arabidopsis glucose signaling and abscisic acid biosynthesis and functions. The Plant Cell **14**, 2723–2743.

Christmann A, Weiler E, Steudle E, Grill E. 2007 A hydraulic signal in root-to-shoot signalling of water shortage. The Plant Journal **52**, 167–174.

Dietz KJ, Sauter A, Wichert K, Messdaghi D, Hartung W. 2000. Extracellular β-glucosidase activity in barley involved in the hydrolysis of ABA glucose conjugate in leaves. Journal of Experimental Botany **51**, 937–944.

Dong T, Xu ZY, Park Y, Kim DH, Lee Y, Hwang I. 2014. ABA UDP-glucosyltransferases play a crucial role in ABA homeostasis in Arabidopsis. Plant Physiology **165,** 277–289.

Endo A, Sawada Y, Takahashi H, Okamoto M, Ikegami K, Koiwai H, Seo M, Toyomasu T, Mitsuhashi W, Shinozaki K, Nakazono M, Kamiya Y, Koshiba T, Nambara E. 2008. Drought induction of Arabidopsis 9-cis-epoxycarotenoid dioxygenase occurs in vascular parenchyma cells. Plant Physiology **147**, 1984–1993.

Endo A, Okamoto M, Koshiba T. 2014. ABA biosynthetic and catabolic pathways. In Abscisic Acid: Metabolism, Transport and Signaling (Zhang, DP, eds). Dordrecht: Springer Science, pp. 21–45.

González-Guzmán M, Apostolova N, Bellés JM, Barrero JM, Piqueras P, Ponce MR, Micol JL, Serrano R, Rodríguez PL. 2002. The short-chain alcohol dehydrogenase ABA2 catalyzes the conversion of xanthoxin to abscisic aldehyde. The Plant Cell **14**, 1833–1846.

Gotté M, Ghosh R, Bernard S, Nguema-Ona E, Vicré-Gibouin M, Hara-Nishimura I, Driouich A. 2015. Methyl jasmonate affects morphology, number and activity of endoplasmic reticulum bodies in *Raphanus sativus* root cells. Plant and Cell Physiology **56**, 61–72.

Han YJ, Cho KC, Hwang OJ, Choi YS, Shin AY, Hwang I, Kim J. 2012. Overexpression of an *Arabidopsis* β-glucosidase gene enhances drought resistance with dwarf phenotype in creeping bentgrass. Plant Cell Reports **31**, 1677.

Hara-Nishimura I, Shimada T, Hatano K, Takeuchi Y, Nishimura M. 1998. Transport of storage proteins to protein storage vacuoles is mediated by large precursor-accumulating vesicles. The Plant Cell **10**, 825–836.

Harris MJ, Dugger WM. 1986. The occurrence of abscisic acid and abscisyl-β- D-glucopyranoside in developing and mature citrus fruit as determined by enzyme immunoassay. Plant Physiology **82,** 339–345.

Hayashi Y, Yamada K, Shimada T, Matsushima R, Nishizawa NK, Nishimura M, Hara-Nishimura I. 2001. A proteinase-storing body that prepares for cell death or stresses in the epidermal cells of Arabidopsis. Plant and Cell Physiology **42**, 894–899.

Herman E, Schmidt M. 2004. Endoplasmic reticulum to vacuole trafficking of endoplasmic reticulum bodies provides an alternate pathway for protein transfer to the vacuole. Plant Physiology **136**, 3440–3446.

Holbrook NM, Shashidhar VR, James RA, Munns R. 2002. Stomatal control in tomato with ABA-deficient roots: response of grafted plants to soil drying. Journal of Experimental Botany **53**, 1503–1514.

Inomata M, Hirai N, Yoshida R, Ohigashi H. 2004. The biosynthetic pathway to abscisic acid via ionylideneethane in the fungus *Botrytis cinerea*. Phytochemistry. **65**, 2667–2678.

Iuchi S, Kobayashi M, Yamaguchi-Shinozaki K, Shinozaki K.

2000. A stress-inducible gene for 9-*cis*-epoxycarotenoid dioxygenase involved in abscisic acid biosynthesis under water stress in drought-tolerant cowpea. Plant Physiology **123**, 553–562.

Iuchi S, Kobayashi M, Taji T, Naramoto M, Seki M, Kato T, Tabata S, Kakubari Y, Yamaguchi-Shinozaki K, Shinozaki K. 2001. Regulation of drought tolerance by gene manipulation of 9-*cis*-epoxycarotenoid dioxygenase, a key enzyme in abscisic acid biosynthesis in *Arabidopsis*. The Plant Journal **27**, 325–333.

Koiwai H, Nakaminami K, Seo M, Mitsuhashi W, Toyomasu T, Koshiba T. 2004. Tissue-specific localization of an abscisic acid biosynthetic enzyme, AAO3, in Arabidopsis. Plant Physiology **134**, 1697–1707.

Kuromori T, Sugimoto E, Shinozaki K. 2014. Intertissue signal transfer of abscisic acid from vascular cells to guard cells. Plant Physiology **164**, 1587–1592.

Kushiro T, Okamoto M, Nakabayashi K, Yamagishi K, Kitamura S, Asami T, Hirai N, Koshiba T, Kamiya Y, Nambara E. 2004. The *Arabidopsis* cytochrome P450 CYP707A encodes ABA 8'-hydroxylases: key enzymes in ABA catabolism. The EMBO Journal **23**, 1647–1656.

Lee KH, Piao HL, Kim HY, Choi SM, Jiang F, Hartung W, Hwang I, Kwak JM, Lee IJ, Hwang I. 2006. Activation of glucosidase via stress-induced polymerization rapidly increases active pools of abscisic acid. Cell **126**, 1109–1120.

Léon-Kloosterziel KM, Gil MA, Ruijs GJ, Jacobsen SE, Olszewski NE, Schwartz SH, Zeevaart JA, Koornneef M. 1996. Isolation and characterization of abscisic acid-deficient Arabidopsis mutants at two new loci. The Plant Journal **10**, 655–661.

Li Q, Ji K, Sun Y, Luo H, Wang H, Leng P. 2013. The role of *FaBG3* in fruit ripening and *B. cinerea* fungal infection of strawberry. The Plant Journal **76**, 24–35.

Lim E-K, Doucet CJ, Hou B, Jackson RG, Abrams SR, Bowles DJ. 2005. Resolution of (+)-abscisic acid using an Arabidopsis glycosyltransferase. Tetrahedron: Asymmetry **16**, 143–147.

Livak KJ, Schmittgen TD. 2001. Analysis of relative gene expression data using real-time quantitative PCR and the $2^{-\Delta\Delta Ct}$ method. Methods **25**, 402–408.

Lymperopoulos P, Msanne J, Rabara R. 2018. Phytochrome and Phytohormones: Working in Tandem for Plant Growth and Development. Frontiers in Plant Science **9**, 1037

Marin E, Nussaume L, Quesada A, Gonneau M, Sotta B, Hugueney P, Frey A, Marion-Poll A. 1996. Molecular identification of zeaxanthin epoxidase of *Nicotiana plumbaginifolia*, a gene involved in abscisic acid biosynthesis and corresponding to the ABA locus of *Arabidopsis thaliana*. The EMBO Journal **15,** 2331–2342.

Matsushima R, Hayashi Y, Kondo M, Shimada T, Nishimura M, Hara-Nishimura I. 2002. An endoplasmic reticulum-derived structure that is induced under stress conditions in Arabidopsis. Plant Physiology **130**, 1807-1814.

Matsushima R, Kondo M, Nishimura M, Hara-Nishimura I. 2003a. A novel ER-derived compartment, the ER body, selectively accumulates a β-glucosidase with an ER-retention signal in *Arabidopsis*. The Plant Journal **33**, 493–502.

Matsushima R, Hayashi Y, Yamada K, Shimada T, Nishimura M, Hara-Nishimura I. 2003b. The ER Body, a novel endoplasmic reticulum-derived structure in *Arabidopsis*. Plant and Cell Physiology **44**, 661–666.

Ma Y, Qin F. 2014. ABA regulation of plant responses to drought and salt stresses. Abscisic Acid: Metabolism, Transport and Signaling, 315–336.

Nagano AJ, Maekawa A, Nakano RT, Miyahara M, Higaki T, Kutsuna N, Hasezawa S, Hara-Nishimura I. 2009. Quantitative analysis of ER body morphology in an Arabidopsis mutant. Plant and Cell Physiology **50**, 2015–2022.

Nakagawa T, Suzuki T, Murata S, Nakamura S, Hino T, Maeo K, Tabata R, Kawai T, Tanaka K, Niwa Y, Watanabe Y, Nakamura K, Kimura T, Ishiguro S. 2007. Improved Gateway binary vectors: high-performance vectors for creation of fusion constructs in transgenic analysis of plants. Bioscience, Biotechnology, and Biochemistry **71**, 2095–2100.

Nakano RT, Piślewska-Bednarek M, Yamada K, Edger PP, Miyahara M, Kondo M, Böttcher C, Mori M, Nishimura M, Schulze-Lefert P, Hara-Nishimura I, Bednarek P. 2017. PYK10 myrosinase reveals a functional coordination between endoplasmic reticulum bodies and glucosinolates in *Arabidopsis thaliana*. The Plant Journal **89**, 204–220.

Nakano RT, Yamada K, Bednarek P, Nishimura M, Hara-Nishimura I. 2014. ER bodies in plants of the *Brassicales* order: biogenesis and association with innate immunity. Frontiers in Plant Science **5**, 73.

Nakazaki A, Yamada K, Kunieda T, Sugiyama R, Hirai MY, Tamura K, Hara-Nishimura I, Shimada T. 2019. Leaf endoplasmic reticulum bodies identified in Arabidopsis rosette leaves are involved in defense against herbivory. Plant Physiology **179,** 1515–1524.

Nambara E, Marion-Poll A. 2005. Abscisic acid biosynthesis and catabolism. Annual Review of Plant Biology **56**, 165–185.

Nanjo T, Kobayashi M, Yoshiba Y, Sanada Y, Wada K, Tsukaya H, Kakubari Y, Yamaguchi-Shinozaki K, Shinozaki K. 1999. Biological functions of proline in morphogenesis and osmotolerance revealed in antisense transgenic *Arabidopsis thaliana*. The Plant Journal **18**, 185–193.

Nishimura N, Sarkeshik A, Nito K, Park SY, Wang A, Carvalho PC, Lee S, Caddell DF, Cutler SR, Chory J, Yates JR, Schroeder JI. 2010. PYR/PYL/RCAR family members are major *in-vivo* ABI1 protein phosphatase 2C-interacting proteins in *Arabidopsis*. The Plant Journal **61**, 290–299.

Ogasawara K, Yamada K, Christeller JT, Kondo M, Hatsugai N, Hara-Nishimura I, Nishimura M. 2009. Constitutive and inducible ER bodies of *Arabidopsis thaliana* accumulate distinct β-glucosidases. Plant and Cell Physiology **50**, 480–488.

Ohkuma K, Lyon JL, Addicott FT, Smith OE. 1963. Abscisin II, an abscission-accelerating substance from young cotton fruit. Science **142**, 1592–1593.

Okamoto M, Kuwahara A, Seo M, Kushiro T, Asami T, Hirai N, Kamiya Y, Koshiba T, Nambara E. 2006. CYP707A1 and CYP707A2, which encode abscisic acid 8'-hydroxylases, are indispensable for proper control of seed dormancy and

germination in *Arabidopsis*. Plant Physiology **141**, 97–107.

Ondzighi-Assoume CA, Chakraborty S, Harris JM. 2016. Environmental nitrate stimulates abscisic acid accumulation in Arabidopsis root tips by releasing it from inactive stores. The Plant Cell **28**, 729–745.

Preston J, Tatematsu K, Kanno Y, Hobo T, Kimura M, Jikumaru Y, Yano R, Kamiya Y, Nambara E. 2009. Temporal expression patterns of hormone metabolism genes during imbibition of Arabidopsis thaliana seeds: a comparative study on dormant and non-dormant accessions. Plant and Cell Physiology **50**, 1786–1800.

Priest DM, Ambrose SJ, Vaistij FE, Elias L, Higgins GS, Ross AR, Abrams SR, Bowles DJ. 2006. Use of the glucosyltransferase UGT71B6 to disturb abscisic acid homeostasis in *Arabidopsis thaliana.* The Plant Journal **46**, 492–502.

Saika H, Okamoto M, Miyoshi K, Kushiro T, Shinoda S, Jikumaru Y, Fujimoto M, Arikawa T, Takahashi H, Ando M, Arimura S, Miyao A, Hirochika H, Kamiya Y, Tsutsumi N, Nambara E, Nakazono M. 2007. Ethylene promotes submergence-induced expression of *OsABA8ox1*, a gene that encodes ABA 8'-hydroxylase in rice. Plant and Cell Physiology **48**, 287–298

Saito S, Hirai N, Matsumoto C, Ohigashi H, Ohta D, Sakata K, Mizutani M. 2004. Arabidopsis *CYP707A*s encode (+)-abscisic acid 8'-hydroxylase, a key enzyme in the oxidative catabolism of abscisic acid. Plant Physiology **134**, 1439–1449.

Schroeder JI, Allen GJ, Hugouvieux V, Kwak JM, Waner D. 2001. Guard cell signal transduction. Annual Review of Plant Physiology and Plant Molecular Biology **52**, 627–658.

Schwarz DS, Blower MD. 2016. The endoplasmic reticulum: structure, function and response to cellular signaling. Cellular and Molecular Life Sciences **73**, 79–94.

Schwartz SH, Tan BC, Gage DA, Zeevaart JAD & McCarty DR. 1997. Specific oxidative cleavage of carotenoids by VP14 of maize. Science **276**, 1872–1874.

Seo M, Peeters A, Koiwai H, Oritani T, Marion-Poll A, Zeevaart J, Koornneef M, Kamiya Y, Koshiba T. 2000. The *Arabidopsis* aldehyde oxidase 3 (*AAO3*) gene product catalyzes the final step in

abscisic acid biosynthesis in leaves. Proceedings of the National Academy of Sciences of the United States of America **97**, 12908–12913.

Sherameti I, Venus Y, Drzewiecki C, Tripathi S, Dan VM, Nitz I, Varma A, Grundler FM, Oelmüller R. 2008. PYK10, a β-glucosidase located in the endoplasmic reticulum, is crucial for the beneficial interaction between *Arabidopsis thaliana* and the endophytic fungus *Piriformospora indica*. The Plant Journal **54**, 428–439.

Shinozaki K, Yamaguchi-Shinozaki K. 2007. Gene networks involved in drought stress response and tolerance. Journal of Experimental Botany **58**, 221–227.

Takagi H, Ishiga Y, Watanabe S, Konishi T, Egusa M, Akiyoshi N, Matsuura T, Mori IC, Hirayama T, Kaminaka H, Shimada H, Sakamoto A. 2016. Allantoin, a stress-related purine metabolite, can activate jasmonate signaling in a MYC2-regulated and abscisic acid-dependent manner. Journal of Experimental Botany **67**, 2519–2532.

Thompson AJ, Jackson AC, Symonds RC, Mulholland BJ, Dadswell AR, Blake PS, Burbidge A, Taylor IB. 2000. Ectopic expression of a tomato 9-*cis*-epoxycarotenoid dioxygenase gene causes over-production of abscisic acid. The Plant Journal for Cell and Molecular Biology **23**, 363–374.

Toyooka K, Okamoto T, Minamikawa T. 2000. Mass transport of proform of a KDEL-tailed cysteine proteinase (SH-EP) to protein storage vacuoles by endoplasmic reticulum-derived vesicle is involved in protein mobilization in Germinating Seeds. Journal of Cell Biology **148,** 453–464.

Urano K, Maruyama K, Ogata Y, Morishita Y, Takeda M, Sakurai N, Suzuki H, Saito K, Shibata D, Kobayashi M, Yamaguchi-Shinozaki K, Shinozaki K. 2009. Characterization of the ABA-regulated global responses to dehydration in *Arabidopsis* by metabolomics. The Plant Journal, **57,** 1065–1078.

Vitale A, Denecke J. 1999. The endoplasmic reticulum-gateway of the secretory pathway. The Plant Cell **11**, 615–628.

Wang XF, Zhang DP. 2014. ABA Signal Perception and ABA

Receptors. In Abscisic Acid: Metabolism, Transport and Signaling (Zhang, DP, eds). Dordrecht: Springer science+Business Media, pp. 89–116.

Watanabe S, Kounosu Y, Shimada H, Sakamoto A. 2014a. Arabidopsis *xanthine dehydrogenase* mutants defective in purine degradation show a compromised protective response to drought and oxidative stress. Plant Biotechnology **31**, 173–178.

Watanabe S, Matsumoto M, Hakomori Y, Takagi H, Shimada H, Sakamoto A. 2014b. The purine metabolite allantoin enhances abiotic stress tolerance through synergistic activation of abscisic acid metabolism. Plant, Cell & Environment **37**, 1022–1036.

Watanabe S, Nakagawa A, Izumi S, Shimada, H, Sakamoto A. 2010. RNA interference-mediated suppression of xanthine dehydrogenase reveals the role of purine metabolism in drought tolerance in Arabidopsis. FEBS Letters **584**, 1181–1186.

Weijers D, Nemhauser J, Yang Z. 2018. Auxin: small molecule, big impact, Journal of Experimental Botany **69**, 133–136.

Werner AK, Witte C-P. 2011. The biochemistry of nitrogen mobilization: purine ring catabolism. Trends in Plant Science **16**, 381–387.

Winter D, Vinegar B, Nahal H, Ammar R, Wilson GV, Provart NJ. 2007. An "Electronic Fluorescent Pictograph" browser for exploring and analyzing large-scale biological data sets. PLoS ONE **2**, e718.

Xiong L, Lee H, Ishitani M, Zhu JK. 2002. Regulation of osmotic stress-responsive gene expression by the *LOS6*/*ABA1* locus in *Arabidopsis*. Journal of Biological Chemistry **277**, 8588–8596.

Xu ZW, Escamilla-Treviño LL, Zeng LH, Lalgondar M, Bevan D, Winkel B, Mohamed A, Cheng CL, Shih MC, Poulton J, Esen A. 2004. Functional genomic analysis of Arabidopsis thaliana glycoside hydrolase family 1. Plant Molecular Biology **55**, 343–367.

Xu ZY, Lee KH, Dong T, Jeong JC, Jin JB, Kanno Y, Kim DH, Kim SY, Seo M, Bressan RA, Yun DJ, Hwang I. 2012. A vacuolar β-glucosidase homolog that possesses glucose-conjugated abscisic acid hydrolyzing activity plays an important role in osmotic stress responses in *Arabidopsis.* The Plant Cell **24**, 2184–2199.

Yamada K, Hara-Nishimura I, Nishimura M. 2011. Unique defense

strategy by the endoplasmic reticulum body in plants. Plant and Cell Physiology **52**, 2039–2049.

Yamada K, Nagano AJ, Nishina M, Hara-Nishimura I, Nishimura M. 2008. NAI2 is an endoplasmic reticulum body component that enables ER body formation in *Arabidopsis thaliana*. The Plant Cell **20**, 2529–2540.

Zeevaart JAD, Creelman RA. 1988. Metabolism and physiology of abscisic acid. Annual Review of Plant Physiology and Plant Molecular Biology **39**, 439–473.

Zhu JK. 2002. Salt and drought stress signal transduction in plants. Annual Review of Plant Biology **53**, 247–273.